

**PEOPLE'S DEMOCRATIC REPUBLIC OF ALGERIA
MINISTRY OF HIGHER EDUCATION AND SCIENTIFIC RESEARCH
M'HAMED BOUGARA UNIVERSITY OF BOUMERDES**



**Faculty of Technology
Mechanical Engineering Department**

Master's Thesis

In pursuit of a **Master's Degree** in Mechanical Engineering

Specialty: Energy Installations and Turbomachinery

Topic:

Calculation and Design of several Scale Models of a Drone

Presented by:

- ZERZOUNI Billel
- ALI AMAR Mokrane

Supervised by:

Dr. GUEMMADI

Academic Year: 2023- 2024

Abstract:

This thesis presents a detailed investigation into the design and analysis of multi-scale drones using MATLAB. The study is structured into three full chapters.

The first chapter provides an in-depth overview of the history, background, and several types of drones. This exploration lays the foundation for understanding the evolution of drone technology and the principles that guide their design and operation.

Chapter II delves into the mathematical underpinnings of drone design. This chapter is divided into two parts: structural and performance parameters. It presents a thorough review of the equations and formulas used in the design process, providing a theoretical framework for the practical application in the subsequent chapter.

Chapter III, applies the theoretical knowledge from chapter two to a practical scenario. Using MATLAB, the structural and performance parameters of a chosen drone, the SKYEYE SIERRA, are calculated. Following this, MATLAB is used to recalculate these parameters for a drone with a different mass, noting the changes in performance and structure. The chapter also includes a study on the effect of the taper ratio on wing design and aerodynamics.

The thesis concludes with the use of SolidWorks for a 3D design of a fixed-wing drone, bringing the theoretical calculations to life. This practical application validates the theoretical calculations and provides a tangible output of the design process.

This research contributes to the field of mechanical engineering by providing a systematic and practical approach to drone design. The methodologies and findings presented in this thesis could guide future research and development in the field of UAVs, particularly in the design of multi-scale drones.

Keywords: Unmanned Aerial Vehicles (UAVs), MATLAB, SolidWorks, Multi-scale drones, Design, Analysis, Structural parameters, Performance, SKYEYE SIERRA, Taper ratio, Wing design, Aerodynamics, Mechanical engineering

Résumé

Cette étude présente une analyse détaillée de la conception et de l'analyse de drones multi-échelles à l'aide de MATLAB. L'étude est structurée en trois chapitres complets.

Le premier chapitre fournit un aperçu approfondi de l'histoire, du contexte et des différents types de drones. Cette exploration pose les bases pour comprendre l'évolution de la technologie des drones et les principes qui guident leur conception et leur fonctionnement.

Le chapitre II se penche sur les fondements mathématiques de la conception des drones. Ce chapitre est divisé en deux parties : les paramètres structurels et de performance. Suivantes un examen approfondi des équations et des formules utilisées dans le processus de conception, fournissant un cadre théorique pour l'application pratique dans le chapitre suivant.

Le chapitre III applique les connaissances théoriques du chapitre deux à un scénario pratique. À l'aide de MATLAB, les paramètres structurels et de performance d'un drone choisi, le SKYEYE SIERRA, sont calculés. Ensuite, MATLAB est utilisé pour recalculer ces paramètres pour un drone d'une masse différente, en notant les changements de performance et de structure. Le chapitre comprend également une étude sur l'effet du rapport de conicité sur la conception de l'aile et l'aérodynamique.

La thèse se conclut par l'utilisation de SolidWorks pour une conception 3D d'un drone à aile fixe, donnant vie aux calculs théoriques. Cette application pratique valide les calculs théoriques et fournit un résultat tangible du processus de conception.

Cette recherche contribue au domaine du génie mécanique en fournissant une approche systématique et pratique de la conception des drones. Les méthodologies et les résultats présentés dans cette thèse pourraient guider la recherche et le développement futurs dans le domaine des UAV, en particulier dans la conception de drones multi-échelles.

Mots-clés : Véhicules aériens sans pilote (UAV), MATLAB, SolidWorks, Drones multi-échelles, Conception, Analyse, Paramètres structurels, Performance, SKYEYE SIERRA, Conception d'ailes, Aérodynamique.

ملخص

تقدم هذه المذكرة بحثاً مفصلاً حول تصميم وتحليل الطائرات بدون طيار متعددة الأحجام باستخدام برنامج حسابي. تتكون الدراسة من ثلاثة فصول شاملة.

يقدم الفصل الأول نظرة عميقة على التاريخ والخلفية والأنواع المختلفة للطائرات بدون طيار. يضع هذا الاستكشاف الأساس لفهم تطور تكنولوجيا الطائرات بدون طيار والمبادئ التي توجه تصميمها وتشغيلها.

يغوص الفصل الثاني في الأساس الرياضي لتصميم الطائرات بدون طيار. ينقسم هذا الفصل إلى جزأين: المعلومات الهيكلية والأداء. يقدم استعراضاً شاملاً للمعادلات والصيغ المستخدمة في عملية التصميم، مما يوفر إطاراً نظرياً للتطبيق العملي في الفصل التالي.

يطبق الفصل الثالث المعرفة النظرية من الفصل الثاني على سيناريو عملي. باستخدام البرنامج الحسابي، يتم حساب المعلومات الهيكلية والأداء لطائرة بدون طيار مختارة، وهي طائرة بدون طيار من نوع معين. بعد ذلك، يتم استخدام البرنامج الحسابي لإعادة حساب هذه المعلومات لطائرة بدون طيار بكتلة مختلفة، ملاحظة التغييرات في الأداء والهيكل. يتضمن الفصل أيضًا دراسة عن تأثير نسبة التدرج على تصميم الجناح والديناميكا الهوائية.

تختتم الرسالة باستخدام برنامج تصميم ثلاثي الأبعاد لطائرة بدون طيار ذات جناح ثابت، مما يجلب الحسابات النظرية إلى الحياة. يُثبت هذا التطبيق العملي الحسابات النظرية ويوفر ناتجًا ملموسًا لعملية التصميم.

الكلمات الرئيسية: الطائرات بدون طيار، برنامج تصميم ثلاثي الأبعاد، الطائرات بدون طيار متعددة الأحجام، التصميم، التحليل، المعلومات الهيكلية، الأداء، طائرة بدون طيار من نوع معين، نسبة التدرج، تصميم الجناح، الديناميكا الهوائية، الهندسة الميكانيكية، MATLAB, SolidWorks.

Table of Contents

Abbreviation list

List of Figures

List of Tables

General introduction[14]

Chapter I: An overview of drones and their background

I.1. Introduction[17]

I.2. Historical Background..... [17]

I.3. Importance and Applications..... [18]

I.3.1 Aerial Photography and Videography.....[18]

I.3.2 Pipeline Inspections and monitoring.....[19]

I.3.3 Package Delivery Services.....[19]

I.3.4 Search and Rescue (SAR) operations[20]

I.3.5. Agriculture and Crop Monitoring.....[22]

I.3.6. Wildfire detection[22]

I.4. Classification of drones.....[23]

I.4.1 According to their structure.....[23]

I.4.1.1 Fixed-wing drones.....[23]

I.4.1.2 Rotary wing drones.....[23]

I.4.2 Depending on the mode of propulsion.....[25]

I.4.2.1 fuel sources.....[25]

I.4.2.2 electric batteries.....[25]

I.4.3 Level of Autonomy.....[25]

I.5. Challenges and Future Prospects.....[26]

I.6. Conclusion..... [26]

Chapter II: Theoretical and mathematical reminder on the calculation of the
structural parameters of a drone

II.1. Introduction.....[28]

II.2. Wing Design Parameters.....	[28]
II.2.1 Wing utility.....	[28]
II.2.2 Wing areab.....	[28]
II.2.3. Aspect ratio.....	[29]
II.2.4. Wing loading.....	[20]
II.2.5 Mean Aerodynamic Chord.....	[31]
II.3. Aircraft stabilizer.....	[32]
II.3.1 The Tail Assembly.....	[32]
II.3.2 Sizing the Stabilizer Surfaces.....	[35]
II.4 Theory of flight.....	[39]
II.5. Steady flight.....	[44]
II.5.1 Pitch axis centering and stability.....	[48]
II.6 Conclusion.....	[49]

Chapter III: Presentation of the model studied and the calculation of its various parameters

III.1 Introduction:	[52]
III.2 SKYEYE SIERRA UAV.....	[52]
III.2.1 Technical details.....	[52]
III.3 Structure (first part of the design process.....	[53]
III.3.1 Wing area.....	[53]
III.3.2 Aspect ratio.....	[54]
III.3.3 Wing loading.....	[55]
III.3.4 Mean Aerodynamic Chord (MAC)	[55]
III.3.5 Mean Aerodynamic Chord location.....	[56]
III.3.6 Aircraft stabilizer.....	[57]
III.3.6.1 Length between the aerodynamic centers of the wing and horizontal tailplane.....	[57]
III.3.6.2 Length between the aerodynamic centers of the wing and vertical tailplane.....	[58]
III.4 Flight Dynamics (second part of the design process)	[59]
III.4.1 Lift and Drag.....	[59]

III.4.2 Number of Reynolds.....	[61]
III.4.3 Weight force.....	[62]
III.4.4 Lift to Drag ratio.....	[62]
III.4.5 AFT CG Limit	[64]
III.5 Effect of mass change on performance	[67]
III.6 Effects of Taper Ratio on Aerodynamic Parameters of fixed wing Drone...	[67]
III.6.1 Material method	[68]
a- Planform Geometry and Aerodynamic Parameters of an Aircraft Wing.....	[68]
b- Numerical Analyses	[69]
c- Results and discussion	[70]
III.6.2 Conclusion	[73]
Organizational Chart	[73]
SolidWorks Drawings.....	[76]
General introduction.....	[81]

Abbreviation List

ACGL	:	Aft Center of Gravity Limit
AR	:	Aspect Ratio
b	:	Wingspan
C _D	:	Coefficient of Drag
CG	:	center of gravity
C _{HT}	:	Horizontal tail volume coefficient
C _L	:	Coefficient of Lift
Cr	:	root chord
Ct	:	tip chord
C _{VT}	:	Vertical tail volume coefficient
FAA	:	Federal Aviation Authority
GA	:	General Aviation
F _D	:	Drag force
F _L	:	Lifting force
L _{HT}	:	Length between the aerodynamic centers of the wing and horizontal tailplane
L _{VT}	:	Length between the aerodynamic centers of the wing and vertical tailplane
MDPI	:	Multidisciplinary Digital Publishing Institute
MAC	:	Mean Aerodynamical Chord
Re	:	Reynolds Number
UAV	:	Unmanned Aerial Vehicle
S _{HT}	:	Horizontal tail area
S _{VT}	:	Vertical tail area
SAR	:	Search And Rescue

U_G : Gust Velocity
 U_R : relative wind
 V_H : Horizontal Speed
VMCA : Minimum Control Speed when Airborne
 V_T : Trajectory Speed
CAD : Computer Aided Design

List of Figures

Chapter I:

<i>Figure I.1</i>	<i>the launch of the Queen Bee radio-controlled target drone, 6 June 1941</i>	<i>18</i>
<i>Figure I.2</i>	<i>Quadcopter during package delivery used by DPD group</i>	<i>20</i>
<i>Figure I.3</i>	<i>Example of a heat map produced by a saliency detection method using a SeaDronesSee</i>	<i>21</i>
<i>Figure I.4</i>	<i>Fixed wing drone</i>	<i>24</i>
<i>Figure I.5</i>	<i>Rotary wing drones</i>	<i>24</i>
<i>Figure I.6</i>	<i>Phantom 4 drone</i>	<i>25</i>
<i>Figure I.7</i>	<i>Hubsan X4</i>	<i>25</i>

Chapter II:

<i>Figure II.1</i>	<i>Surface area of a trapezoidal wing</i>	<i>29</i>
<i>Figure II.2</i>	<i>Aspect ratio of a rectangular wing</i>	<i>29</i>
<i>Figure II.3</i>	<i>Aspect ratio of a trapezoidal wing</i>	<i>30</i>
<i>Figure II.4</i>	<i>MAC of swept back wing</i>	<i>32</i>
<i>Figure II.5</i>	<i>A Cessna 172 with the Horizontal and Vertical Stabilizer Labelled</i>	<i>33</i>
<i>Figure II.6</i>	<i>Example of the response to an upward gust of an aircraft that is Longitudinal Statically Stable</i>	<i>34</i>
<i>Figure II.7</i>	<i>Downward acting normal force on the horizontal stabilizer in a conventional arrangement</i>	<i>34</i>
<i>Figure II.8</i>	<i>Contribution of the vertical stabilizer to yaw (directional) stability</i>	<i>35</i>
<i>Figure II.9</i>	<i>Tail Volume Coefficient Variables</i>	<i>36</i>
<i>Figure II.10</i>	<i>The four aerodynamic forces applied on wing profile</i>	<i>40</i>
<i>Figure II.11</i>	<i>The variation of C_D and C_L with the angle of attack</i>	<i>41</i>
<i>Figure II.12</i>	<i>Drag polar curve</i>	<i>42</i>
<i>Figure II.13</i>	<i>Variation of drag polar curves with different Reynolds numbers</i>	<i>44</i>

<i>Figure II.14</i>	<i>The four aerodynamic forces acting on an aircraft</i>	<i>45</i>
<i>Figure II.15</i>	<i>Force vectors during a stabilized climb</i>	<i>45</i>
<i>Figure II.16</i>	<i>Pitching moment model on CG and center of pressure</i>	<i>48</i>

Chapter III:

<i>Figure III.1</i>	<i>The ElevonX SKYEYE DRONE</i>	<i>53</i>
<i>Figure III.2</i>	<i>Trapezoidal wing area</i>	<i>54</i>
<i>Figure III.3</i>	<i>Locating the Mean Aerodynamic Chord using the drawing method</i>	<i>56</i>
<i>Figure III.4</i>	<i>Lift and drag aerodynamic forces on a wing profile</i>	<i>60</i>
<i>Figure III.5</i>	<i>Drag curve for light aircraft. The tangent gives the maximum L/D point</i>	<i>63</i>
<i>Figure III.6</i>	<i>Trajectory speed</i>	<i>63</i>
<i>Figure III.7</i>	<i>Aircraft wing root and tip chords</i>	<i>68</i>
<i>Figure III.8</i>	<i>Planform geometries of revised wing models</i>	<i>69</i>
<i>Figure III.9</i>	<i>Reynolds Number versus taper ratios of the models</i>	<i>71</i>
<i>Figure III.10</i>	<i>Induced drag parameters (δ) versus taper ratios of the models</i>	<i>71</i>
<i>Figure III.11</i>	<i>Induced drag parameter versus taper ratio and aspect ratio</i>	<i>72</i>
<i>Figure III.12</i>	<i>Induced drag coefficients versus taper ratios of the models</i>	<i>72</i>
<i>Figure III.13</i>	<i>Organizational Chart of the MATLAB program</i>	<i>75</i>
<i>Figure III.14</i>	<i>3D back view of the designed drone</i>	<i>76</i>
<i>Figure III.15</i>	<i>3D front view of the designed drone</i>	<i>77</i>
<i>Figure III.16</i>	<i>3D upper view of the designed drone</i>	<i>77</i>

List of Tables

Chapter I: (No Tables)

Chapter II:

<i>Table II.1</i>	<i>List of Recommended Horizontal Stabilizer (tail) Volume Coefficient</i>	<i>37</i>
<i>Table II.2</i>	<i>List of Recommended Vertical Stabilizer (tail) Volume Coefficients</i>	<i>38</i>

Chapter III:

<i>Table III.1</i>	<i>Technical details of the SKYEYE SIERRA</i>	<i>53</i>
<i>Table III.2</i>	<i>Giving data for the calculation of the structural parameters</i>	<i>58</i>
<i>Table III.3</i>	<i>Calculated structural parameters</i>	<i>59</i>
<i>Table III.4</i>	<i>Giving data for the calculation of the performance parameters</i>	<i>65</i>
<i>Table III.5</i>	<i>Calculated performance parameters of the 17.5 kg drone</i>	<i>66</i>
<i>Table III.6</i>	<i>Calculated performance parameters of the 5,6 kg drone</i>	<i>67</i>
<i>Table III.7</i>	<i>Geometrical dimensions of the models</i>	<i>69</i>

General Introduction

General Introduction

In the rapidly evolving field of unmanned aerial vehicles (UAVs), commonly known as drones, the integration of advanced computational tools is essential for the development of efficient and reliable systems. This thesis presents a comprehensive approach to drone design, emphasizing the automation of parameter calculations.

To contextualize this work, it is important to understand the historical evolution of UAVs. The concept of unmanned flight dates back to the mid-19th century, with the first recorded use of an unmanned aerial vehicle for warfare occurring in July 1849. However, the first true UAVs, capable of successful return after a mission, were developed in the late 1950s.

Throughout the 20th century, UAVs were primarily developed for military missions deemed too “dull, dirty or dangerous” for humans. By the 21st century, as control technologies improved and costs fell, the use of UAVs expanded to many non-military applications.

This historical perspective underscores the significant advancements in UAV technology and the increasing importance of computational tools in their design and operation. The present thesis contributes to this ongoing evolution by offering a streamlined and efficient approach to drone design, facilitated by the use of MATLAB for automated parameter calculations. This work aims to further the development of UAVs, enhancing their efficiency, reliability, and applicability in various sectors.

The objective is to develop a MATLAB program capable of dynamically adjusting the drone’s parameters in response to changes in its mass and study the effect of the Taper Ratio (λ) on the wing aerodynamic parameters. This automation is crucial for optimizing the drone’s performance across various payloads and operational conditions. By establishing a mathematical model that encompasses the drone’s physical characteristics and flight dynamics, we can simulate and analyze the behavior of the drone under different scenarios.

The significance of this work lies in its potential to streamline the design process, reduce the time and cost associated with iterative testing, and enhance the adaptability of drones to specialized tasks. The methodology adopted in this thesis could serve as a blueprint for future UAV design projects, where precision and adaptability are paramount.

As we embark on this exploration of drone design and MATLAB automation, we anticipate uncovering insights that will propel the field of UAV technology forward, paving the way for more sophisticated and versatile aerial platforms.

To obtain our objective, we decided to split this work into three parts: 1. chapter I. An overview of drones and their background, 2. Chapter II. Theoretical and mathematical reminder on the calculation of the structural parameters of a drone, 3. Chapter III. Presentation of the model studied and the calculation of its various parameters.

- In the first chapter, we go through the history, evolution and developments that drones passed by to become an essential part in this modern world, mentioning their vast and significant use, different classifications of UAVs and some challenges in the days to come.

- The second chapter is more of a reminder of different mathematical equations used in flight mechanics calculations (structure) and performance determination (aerodynamics), aircraft design, we will be explaining along the way how we use these equations in a simple manner.
- The third chapter is the highlight of our work, we will present in detail the results of the different laws already explained in the previous chapter and we will reveal the MATLAB program used to do the same calculations but with different masses and compare the two methods results. Then, we will see the effect of the Taper Ratio (λ) on the drone wing aerodynamic parameters. Finishing the study by a 3D module and different projections using SolidWorks software.

Finally, we will summarize this work with a general conclusion in which we encapsulate the key findings, discuss the implications of our research, and suggest potential directions for future work in the field of Unmanned Aerial Vehicle (UAV) design. We will also reflect on the challenges encountered during the research process and how they were addressed, thereby providing valuable insights for future research endeavors. This conclusion will not only wrap up our current work but also pave the way for further advancements in UAV design and technology.

Chapter I

***An overview of drones and their
background***

I.1 Introduction

Drones are the new millennium technology which is going to change the perspective of visualizing things. The phrase 'drones' is also known as 'Unmanned Aerial Vehicle' or 'Unmanned Aerial System'. These are the aircraft that can fly without a human on board. This aircraft will be controlled by an onboard computer or by the remote control of a pilot on the ground. The advancement in technology will come across many types of UAVs. The classification of drones can be done based on their mission requirements. The common types of drones are: Fixed Wing Type, Helicopter Type, and Mini UAVs.

Drones are very critical to modern-day warfare for two central questions: firepower and reducing the risk of human life. During the First Gulf War, there was a large focus on technology to fight against a daunting foe. The CIA used the Pioneer RPV for its first time in combat: over 100 flights were performed in the span of two weeks, providing intelligence for the destruction of a great deal of Iraqi armor and artillery. The importance of drones can be realized with the fact that the U.S. Air Force now trains more pilots for UAVs than for normal fighters and bombers [1].

I.2 Historical Background

Drones have been in place for over a hundred years. The concept of unmanned aircraft dates to 1916 when the US Navy and the Curtiss Airplane and Motor Company developed a pilotless aircraft designed to bomb German submarines. The drone did not appear to be cost-effective, and the use of drones was dropped. Another simpler explanation can be taken from the example of Nazis where they have utilized a blend of multiple bombs to make it a precision-guided weapon.

The progress of UAV technology in the US slowed down after the World War since there was no new rise of potential threats and the shift in military and political priorities. Development and research in drones were alive only in the current conflict of interest.

in 1934, the British Air Ministry took the initiative to develop a new UAV which was again to be used as a weapon. This was to be done by the newly established "special duty flight" at the Royal Aircraft Establishment (RAE). This new aircraft was named the "Queen Bee". This was the first time that the term "drone" was used to describe a UAV, and hence the term has stuck ever since.

Queen Bee was a long-range, high-speed, radio-controlled target aircraft. It had a successful design and served as the prototype for a series of target aircraft that were used for the next 20 years.

This aircraft led to a modern new era for UAVs. During the Second World War, significant progress was made in guided weapons using the Queen Bee as a basis. The Queen Bee and its descendants continued to use a piston and internal combustion engine until the mid-1970s. This was still a beginning phase for UAVs, and a lot had to be developed. By the end of World War II,

it was quite clear that guided weapons were a valid military option. This urged the development of several new types of guided UAVs [2].



Figure I.1 the launch of the Queen Bee radio-controlled target drone, 6 June 1941 [3]

The first mass production of UAVs dates to the early 1980s, and today we see that there are various manufacturers involved in the production of drones.

I.3. Importance and Applications

I.3.1 Aerial Photography and Videography

Photography and videography have greatly benefited from drones, developing an easy way of getting a unique aerial perspective. There are various techniques in which drones have positively influenced producing images and footage from above. In the early days, the quickest method to acquire an aerial perspective was to employ a fixed-wing aircraft, sometimes using a helicopter. Now, offering the same perspective is as easy as activating a drone and flying it to the desired location. The least expensive method for obtaining aerial footage would be to use a camera, doing a flyover of an area and taking still shots. This is not very efficient or effective and doesn't offer a video perspective [4].

By attaching a camera to a drone, one can fly to the specific area needed and videos can be taken along the flyover, offering a more effective video perspective of an area. The video and

photography quality are another aspect where drones have made a huge leap. The popularity of camera drones has taken off in the previous years. Now to have a decent drone with a quality camera, it can cost anywhere from \$800 for a drone such as the undesirable 3DR Solo or reach all the way to \$1,600 for a DJI Inspire 1. With product cost including additional camera gear and other supplies needed to operate the drone, it can quickly turn into an expensive venture. Despite some of the costs, having access to a drone is a cheaper alternative to hiring a professional to obtain aerial footage by using a fixed-wing aircraft or worse, a helicopter [4].

I.3.2 Pipeline Inspections and monitoring

The oil and gas industry relies on an extensive network of pipeline infrastructure to transport crude oil and natural gas across the country. Regular inspection of these pipelines is crucial for detecting leaks, preventing accidents, and avoiding environmental disasters. However, accessing and inspecting buried pipelines manually can be challenging and time-consuming, especially in the desert.

these unmanned aerial vehicles offer significant advantages over traditional methods:

1. **Efficiency:** Drones can cover long distances quickly, reducing the time required for inspections. They fly over pipeline routes, capturing high-resolution images and videos.
2. **Safety:** Drones provide a safer way to inspect difficult-to-reach or dangerous locations along the pipeline. Instead of sending human inspectors into hazardous areas, drones can navigate through tight spaces, over rugged terrain, and even fly above bodies of water.
3. **Consistent Data Collection:** Drones can be preprogrammed to follow exact navigation points and routes, ensuring consistent data collection. They capture visual information, thermal imagery, and other relevant data.
4. **Monitoring Safety Protection Belts:** Drones equipped with visible light pods and mapping equipment can monitor safety protection belts around oil and gas pipelines. They detect illegal facilities, changes in terrain, and potential intrusions.

I.3.3 Package Delivery Services

Companies explore drone delivery options for faster and more efficient last-mile delivery. Amazon.com announced on 1 December 2013 that it was planning a new drone-based delivery service, called Amazon Prime Air. Amazon aims to use a new and more advanced technology platform for delivering packages to customers in 30 minutes or less. A drone in this operation will fly around 400 ft above the ground and carry Products up to five pounds. According to a reliable source, approximately 86% of Amazon's deliveries are under five pounds, so this is a very feasible concept for them. When a customer makes a purchase, an alert will be sent to the nearest distribution center where a drone will confirm the order, then travel to the location of the item and proceed to make the delivery. Essentially, this operation will greatly decrease delivery

time, the need for a transportation service, and packaging cost. Timewise, it is a significant difference, given that any standard shipping method would take 3-5 business days to deliver a product. The standard Amazon Prime shipping means it's delivered within 2 days, but with Amazon Prime Air, you can get your product in 30 minutes. Kay said, "I don't think the FAA is used to working on things that will be out in the consumer's hands in a matter of 4-5 years. 10 years is kind of their timeframe when they implement something like that because they don't want to take any risks. But there's so much upside with unmanned aircraft, the services can be so cost-effective and efficient that it's going to be hard to turn back." He makes a good point. The FAA is known to be slow with changes towards aviation laws, but with a potential upside, they will have to change their outlook and decision-making on drone laws [5].



Figure I.2: Quadcopter during package delivery used by DPD group [6].

I.3.4 Search and Rescue (SAR) operations

Search and Rescue are critical endeavors that involve finding missing individuals, often in challenging or hazardous conditions. Drones have emerged as invaluable tools for enhancing SAR efforts.

The use of drones significantly enhances the effectiveness and safety of rescue missions by providing rapid response, situational awareness, and the ability to access challenging terrains. Their

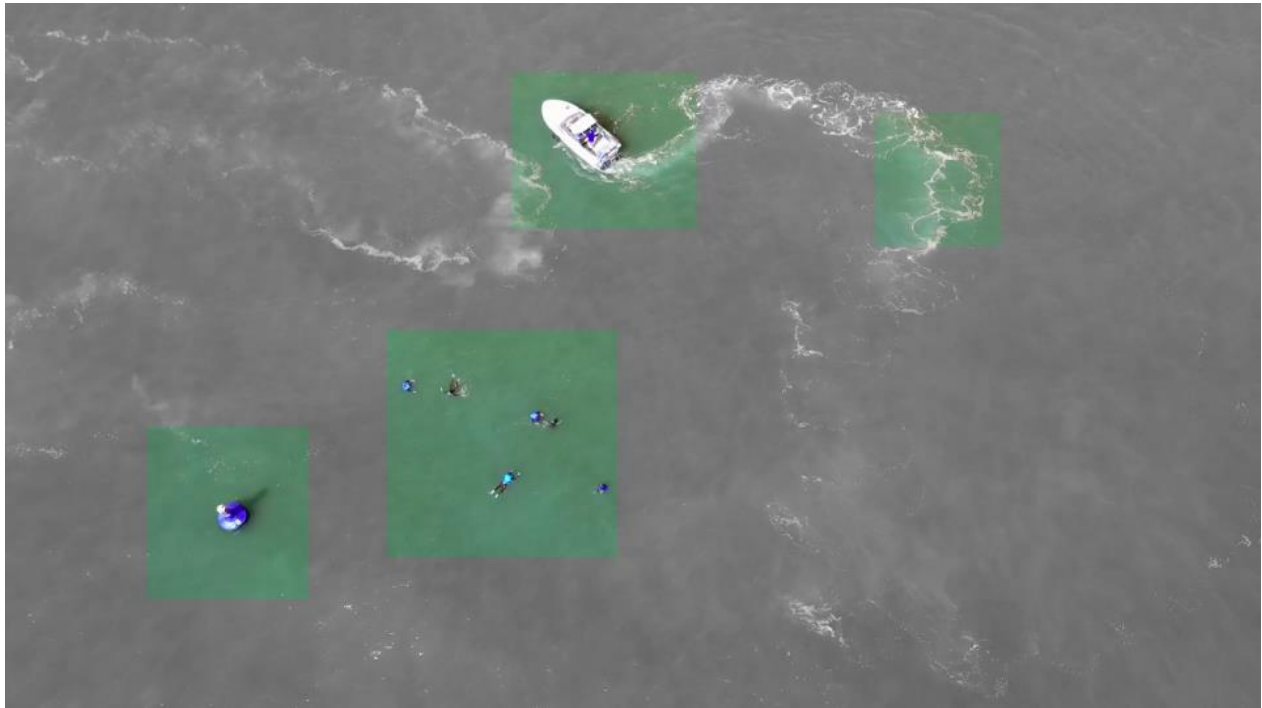


Figure I.3 Example of a heat map produced by a saliency detection method using a SeaDronesSee [7]

versatility and advanced technology make them invaluable assets in saving lives during critical situations.

Here are some key uses and advantages of search and rescue drones:

1. Enhancing Visibility in Challenging Terrains:

- One key advantage of search and rescue drones is their ability to navigate challenging terrains with ease.
- Drones can cover vast areas quickly, especially in rugged landscapes or dense forests.
- They provide aerial views, allowing responders to assess the situation and plan rescue strategies effectively.

Efficiency and Safety in Rescue Missions:

- The integration of drones accelerates rescue missions.
- Drones complement traditional methods and expand capabilities.

2. Mapping Disaster Zones:

- They offer an extensive amount of information at a quicker pace, which can be crucial in life-or-death situations.
- According to a study conducted by DJI EENA, and Black Channel, teams with drones were able to locate victims an average of almost three minutes faster than those operating exclusively on foot [8].

3. Mapping Disaster Zones :

- Drones can rapidly map disaster areas, providing a full understanding of the surrounding terrain.
 - Depending on the camera payload and software, they can create 2D maps, 3D topographic models, or thermal maps [8].
4. **Communication Relay and Situational Awareness:**
- Drones relay messages to individuals once they are found.
 - They keep personnel at a safe distance while efficiently building situational awareness for responders.

Here are some real-life examples of successful Search and Rescue (SAR) drone missions:

1. **Hurricane Harvey (Houston, Texas, 2017) :**

- After Hurricane Harvey caused widespread flooding, drones were deployed to search for hotspots and areas where fires were still burning. They provided real-time information to firefighters and rescue teams on the ground [9].

2. **Hikers in California (San Gabriel Mountains, 2020):**

- Two hikers wandered off the trail in California's San Gabriel Mountains. Drones were instrumental in locating and rescuing them, even in challenging terrain [9].

I.3.5. Agriculture and Crop Monitoring

One of the main uses for drones in agriculture is crop monitoring. It may be a few acres of recreational farming or vast amounts of land that farms certain crops. In order to guarantee a healthy crop free from pests and disease, it is crucial to ensure high crop yields. However, large-scale farms may face difficulties as they often employ workers to manually inspect crops for issues, which can be costly. Additionally, identifying problem areas across vast crop fields poses its own challenges. It is important to ensure that the crop is healthy and is not being affected by pests or disease. Larger farms that employ workers to manually check crops for problem areas can be expensive. It can also be hard to notice problem areas in crops that span large distances.

Drones provide an easier, cheaper, and more efficient way to monitor crops. Drones equipped with near-infrared cameras are able to take detailed pictures of a crop, and the camera software can then process these images to create a heat map. The map will provide information on crop health, where healthy plants reflect more light, and the map will show areas where light is not being reflected, pinpointing possible troubled areas [10].

I.3.6. Wildfire detection

On July 24th, 2023, around 35 wildfires have been rapidly spreading across the northeastern region of Algeria in more than 11 regions causing extensive devastation. The disaster has had a profound impact on 6,000 families, with the Algerian Government reporting 34 confirmed deaths. The affected population heavily relies on crops and livestock, both of which have been severely impacted by the wildfires, resulting in further hardships for the communities. Many homes have been reduced to ashes, leaving families displaced and vulnerable. The dire situation has also affected the health of the population, as the flames and smoke have led to thousands of injuries. The magnitude

of the disaster requires urgent attention and support to address the immediate needs of those affected. However, the prevailing weather conditions remain a cause for concern. With temperatures exceeding 45 degrees Celsius and wind speeds exceeding 50 km/h on the Tunisian borders, coupled with low humidity, the conditions continue to favor the expansion and intensification of the wildfires [11].

The wildfires and heatwaves that swept the country caused a lot of damage to both people and wildlife in Algeria. If we had used drones to detect wildfires at early stages by providing rapid response, efficient coverage, and accurate data. Their deployment could have saved lives and minimized damage during fire emergencies because:

- Drones equipped with thermal cameras and high-resolution sensors can detect wildfires at an early stage.
- They cover large areas quickly, providing real-time information to fire management teams.
- Unlike satellite-based detection, drones are not hindered by cloud cover.

To conclude, the value of any innovation or technology is measured by how useful it is in everyday life, the effect it has on society and the advantages it offers to the user. In the decade, despite being mainly used for military purposes at first, drones have discovered many new applications. Drones have been used for what we discussed above and many other helpful purposes such as real estate, policing, disaster relief, Terrain Mapping, Livestock Management and even internet services.

I.4. Classification of drones

I.4.1 According to their structure

Firstly, drones are classified according to their structure or shape, and two basic distinctions can be made:

Fixed wing

Rotary-wing

I.4.1.1 Fixed-wing drones

Fixed-wing drones are those that use aerodynamics for lifts. They are similar in composition to airplanes, with an elongated body and wings, which emerge from the central main body, generating the lift force in the air.

The advantages of fixed-wing drones are that they are typically more energy efficient than rotary-wing drones, making them ideal for long-range and long duration flights.

Among their main uses, this category of drones is used for photogrammetry, precision agriculture and surveillance, among others. They are capable of covering large areas in a single flight and can be equipped with special cameras and sensors to collect data and generate high-resolution 3D maps and models.



Figure I.4 Fixed wing drone [12]

I.4.1.2 Rotary wing drones

Among the types of UAVs, rotary wing drones or multi-rotors stand out. They are the most common in the current market due to their versatility, which achieve their lift by means of propellers driven by motors located on each of their arms.

This type of drone is quite stable, so they are widely used for all kinds of activities. From light shows with drones, surveillance systems, security and emergency interventions, or even aerial recordings for film and television.



Figure I.5 Rotary wing drones [13]

I.4.2 Depending on the mode of propulsion

The design of drones is dependent upon the energy source that is to be used.

I.4.2.1 Fuel sources

The fuel sources currently available for drones are traditional airplane fuel, battery cells, and fuel cells. Airplane fuel, such as kerosene, is mainly used for large, fixed wing drones. The military Predator drone is one such example of these types of drones. The US army used these drones, and equipped them with different sensors, and ammunition.

I.4.2.2 Electric batteries

Lithium polymer batteries are usually used on smaller multirotor drones. These drones have a shorter range, and smaller operating time than fixed wing drones. Recreational use is a common application for these drones, making it practical to use rechargeable batteries. The Phantom 4 and Hubsan X4 are an example of these types of drones.



Figure I.6 Phantom 4 drone [14]



Figure I.7 Hubsan X4 [15]

I.4.3 Level of Autonomy

Since drones do not carry a pilot on the aerial platform, they need to have a certain level of autonomy. There is a distinction to be made between an automatic and an autonomous system. An automatic system is fully pre-programmed that can execute the programmed task on its own. Automation also includes additional aspects such as automatic flight stabilization.

An Autonomous system can deal with unexpected situations by using preprogrammed rules to decide up a course of action. Automatic systems do not have this freedom of choice [16].

I.5 Challenges and Future Prospects

The future is unpredictable. A constantly moving global society will no doubt present new challenges and opportunities that will impact the future use of drones. Some of these challenges will be technological, some social, and others political. The following discusses these challenges and suggests ways in which they can be met. It must be realized that many of these issues are interrelated and a solution to one may implicitly affect the resolution of another.

An example is the current progress towards more autonomously intelligent drones, which is a double-edged technological sword. This is because, on one hand, greater autonomy can allow more efficient and effective drones in both military and civilian applications. These can range from targeted missile-firing drones to surveying the spread of pollutants.

On the other hand, such drones pose greater safety risks if things go wrong. A missile-firing drone is an obvious safety risk if it malfunctions or falls into the wrong hands. An autonomously intelligent pollution surveying drone may inadvertently spread pollution by failing to distinguish between pollutant and non-pollutant.

Because of the severity of potential risks, it is important that progress towards this kind of technology is met with adequate risk assessment methods and failsafe mechanisms, yet there is no guarantee that this will be the case. Usually, technological failure in a new field is what drives the development of safety mechanisms (an example from aviation being the development of pressurized cockpit doors as a response to modern terrorist threats). This occurs only after a severe incident has taken place, and thus it can be said that one of the fundamentals for safe autonomously intelligent drones is a series of failures concluding in a wake-up call to the developers, by which time much money and damage may have been incurred. This is, in fact, a potential scenario to stop development in this area due to its high risks.

Another interrelated issue is that as safer autonomous drones become a reality, the cost of human casualties in many environments where drones can be used may become increasingly intolerable. This could cause backlash from drone operators facing a reluctance restrictive legislature on autonomous drone use. Ultimately, regression to less autonomous drone systems may be the best compromise between risk and capability in the long-term future.

I.6 Conclusion

This chapter demonstrated that drones are a remarkable product of human creativity and technological advancement. From ancient balloon explosives to modern quadcopters, drones have changed the way we discover our world. As they keep improving, their influence on various areas from security to amusement will only increase. So, the next time you spot a drone flying above, think of its long history and the many inventions that made its existence possible.

Chapter II

***Theoretical and mathematical reminder
on the calculation of the structural
parameters of a drone***

II.1. Introduction

The creation of a flying model involves three stages: design, construction, and piloting. Although most aeromodellers master the last two phases, the design is often left aside due to lack of information. And yet, what satisfaction it is to fly a model from your own imagination! The method proposed here is based on the laws of flight mechanics. Even if these physical laws will not be used directly, a minimum of knowledge of mathematics is necessary for a good understanding.

The formulas used for the calculations are as simple as possible. The same goes for the technical terms used, belonging to basic aeronautical vocabulary.

You should therefore find your way around without too much difficulty, even if you are a beginner in design. You have understood: this method is intended to be Simple, Practical and Performant (S.P.P., that's its name) [17].

It applies to all "classic formula" monoplane aircraft, everything that flies except biplanes, triplanes, Deca planes, Canard formulas, rockets... and intergalactic ships.

First part: structure

The structure of a small aircraft is composed of several main components that support the loads and stresses generated by the aerodynamic forces and the weight of the aircraft. These components include the fuselage, the wings, which provide lift and stability; the empennage, which consists of the horizontal and vertical stabilizers and the control surfaces; and the landing gear, which enables the aircraft to take off and land safely. The design of the structure of a small aircraft must consider the balance between strength, weight, and cost, as well as the performance and safety requirements of the intended mission.

II.2 Wing Design Parameters

The aircraft's wing is probably when of the most important part of the aircraft structure. We should take time to study and cover as much as we can the different parameters in wing design.

II.2.1 Wing utility:

An aircraft's wing is the primary contributor to its ability to generate a lifting force greater than its weight, and therefore take flight.

If you've spent any time looking at pictures of airplanes or taken a walk around an airport you may have noticed that there is an enormous variation in the size and shape of the wings attached to each aircraft. Every wing is carefully sized to best fulfill the mission specifically intended for that airplane or UAV.

II.2.2 Wing area:

With a fixed wingspan, a giving root and tip chords for a slightly swept trapezoidal wing, the wing

area will be calculated using the equation (1) [18]:

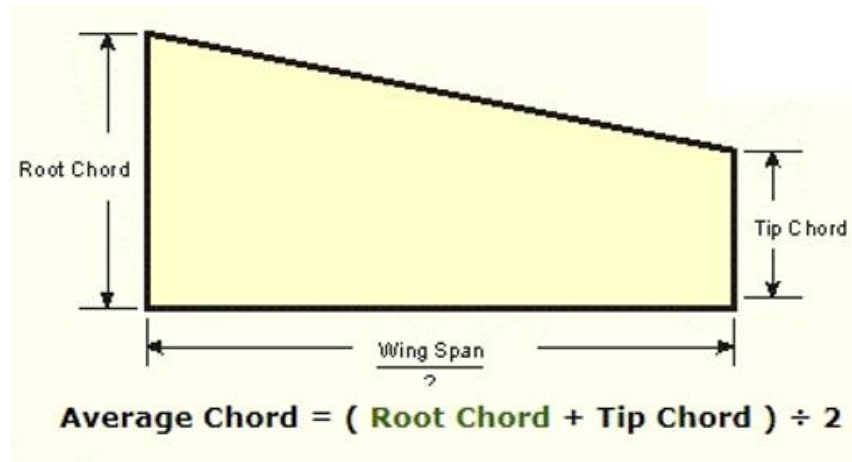


Figure II.1 Surface area of a trapezoidal wing [18].

$$\text{Area} = b \times \frac{(Cr+Ct)}{2} \dots\dots\dots (1)$$

b: wingspan (m)

Cr: root chord (m)

Ct: tip chord (m)

Also, leave a space between the two half-wings as wide as the fuselage (determine this width according to the arrangement of the elements on board the fuselage).

II.2.3 Aspect ratio:

Aspect ratio is the ratio of the wingspan to the mean chord of the wing. It is a measure of how long and slender wings are. A higher aspect ratio means less induced drag and more aerodynamic efficiency. To determine the aspect ratio, we can use the following formula [19]:



Aspect Ratio: $AR = \frac{b}{c} = \frac{b}{c} \times \frac{b}{b} = \frac{b^2}{A}$

Figure II.2 Aspect ratio of a rectangular wing [19].

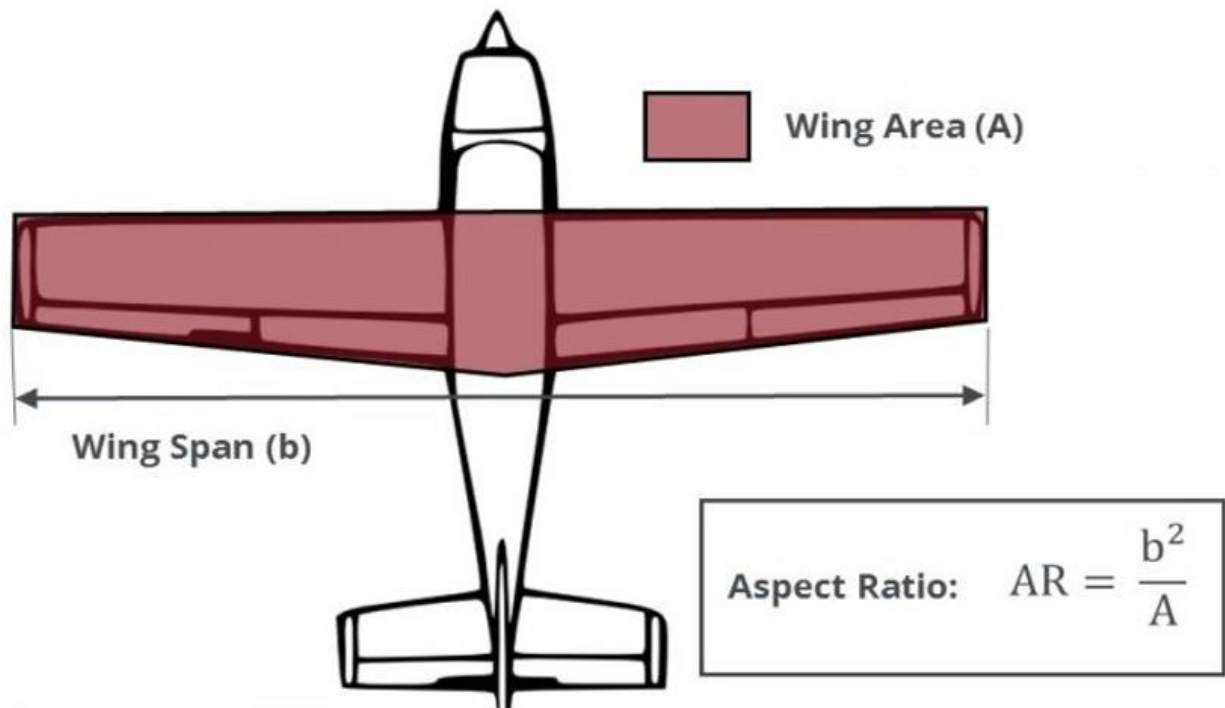


Figure II.3 Aspect ratio of a trapezoidal wing [19].

$$AR = \frac{b^2}{A} \dots\dots\dots (2)$$

where b is the wingspan and Area is the wing area. Substituting the values given in the, we get:

$$AR = (b)^2 / (b \times (C+c) / 2)$$

which simplifies to:

$$AR = (b+c) / (C+c)$$

AR: aspect ratio

A: wing area (m²)

b: wingspan (m)

C: root chord (m)

c: tip chord (m)

II.2.4 Wing loading:

You can tell a great deal about how a bird lives or what an airplane has been designed for just from its wing shape and size. The wings of both birds and planes determine how they might perform or what they might be capable of (for example, gliding, sustained high speed or maneuverability). One way in which the size of the wing can be described is through wing loading.

Wing loading is a measurement that relates the mass of an aircraft or bird to the total wing area. The relationship between wing area and body weight is given in kilograms per square meter (or grams per square centimeter).

If a bird or plane has a low mass but has rather large wings, it will have low wing loading, for example, gliders have low mass with large wings and therefore have low wing loading.

A bird or plane with large body mass and small wings consequently has high or heavy wing loading. An Airbus A380 has a large mass with comparatively small wings. It has heavy wing loading.

To calculate wing loading, divide the mass of the bird or plane by the total area of the upper surface of its wings: wing loading = body mass (kg)/wing area (m²) [19].

$$n = \frac{M}{A} \quad \dots\dots\dots (3)$$

n: Wing loading (kg/m³)

M: Aircraft mass (kg)

A: Wing Area (m²)

II.2.5 Mean Aerodynamic Chord (MAC):

MAC, or Mean Aerodynamic Chord, is the average chord length of a wing. The chord length is the distance from the leading edge to the trailing edge of the wing at a given cross-section.

MAC is calculated by integrating the chord length over the span of the wing and dividing it by the span. MAC is an important parameter for airplanes because it affects the center of pressure, the aerodynamic center, and the moment of inertia of the wing.

MAC also determines the position of the neutral point, which is the point where the pitching moment coefficient is zero. The neutral point is used to define the static margin, which is a measure of the stability of the airplane. The larger the static margin, the more stable the airplane is. Therefore, MAC plays a key role in the design and performance of airplanes.

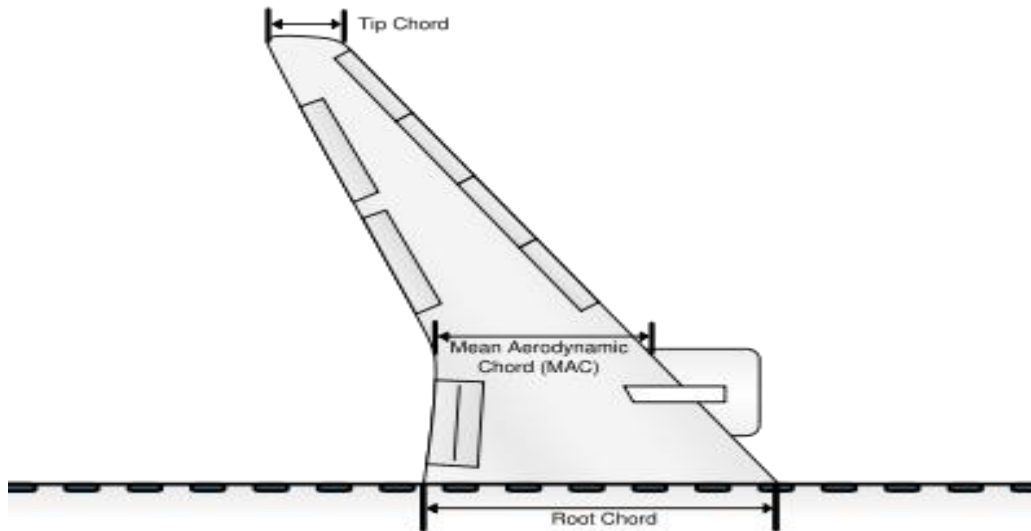


Figure II.4: MAC of swept back wing [17].

The computation of MAC is simple if the aircraft wing has a constant chord; however, this situation is almost never the case because it is often advantageous to introduce taper or sweep into the wing planform. For a linearly tapered (trapezoidal) wing, the MAC equation is presented as follows [17]:

$$MAC = \frac{2}{3} \times \frac{Cr^2 + Cr \times Ct + Ct^2}{Cr + Ct} \quad \dots\dots\dots (4)$$

Where:

MAC: Mean Aerodynamic Chord (m)

Cr: root chord (m)

Ct: tip chord (m)

In addition to the length of the mean aerodynamic chord, its location must be determined.

$$D = \frac{1}{3} \times \frac{(Cr + 2Ct)}{(Cr + Ct)} \times f \quad \dots\dots\dots (5)$$

D: distance or location of the MAC (m)

Cr: root chord (m)

Ct: tip chord (m)

f: sweep angle

II.3. Aircraft stabilizer:

Now we move on to the aircraft tail section and examine the function of both the horizontal and vertical tail. We'll then introduce a practical method to size both surfaces on a new aircraft design. Almost all aircraft flying today have a tail located towards the rear of the fuselage. While there are several possible tail configurations, the majority are comprised of a horizontal surface and a vertical surface which stabilize the aircraft in the longitudinal and directional axis respectively.



Figure II.5 A Cessna 172 with the Horizontal and Vertical Stabilizer Labelled [19]

II.3.1 The Tail Assembly

The tail assembly (horizontal and vertical stabilizer) is also known as the empennage which ensures that the aircraft remains stable through all phases of operation.

An aircraft tail has two primary objectives:

- To provide stability in the longitudinal (pitch) and directional (yaw) axes during flight.
- To assist in the pitch and yaw control of the aircraft by the movement of control surfaces affixed to the stabilizing surfaces.

Horizontal Stabilizer

To understand why a conventional aircraft requires a horizontal stabilizer one only needs to plot the force vectors acting on the aircraft during flight.

An aircraft with the horizontal stabilizer at the rear of the fuselage will always be designed such that the center of gravity (CG) sits ahead of the wing's center of lift. The wing therefore imparts a nose-down pitching moment on the aircraft, the magnitude of which is the resulting lift force multiplied by the moment arm between the center of lift and the CG. This is a deliberate design as it means that any time the aircraft's nose pitches up, the wing will provide a restorative moment that will tend to bring the nose back down. This is termed longitudinal static stability and is the hallmark of a safe and stable airplane.

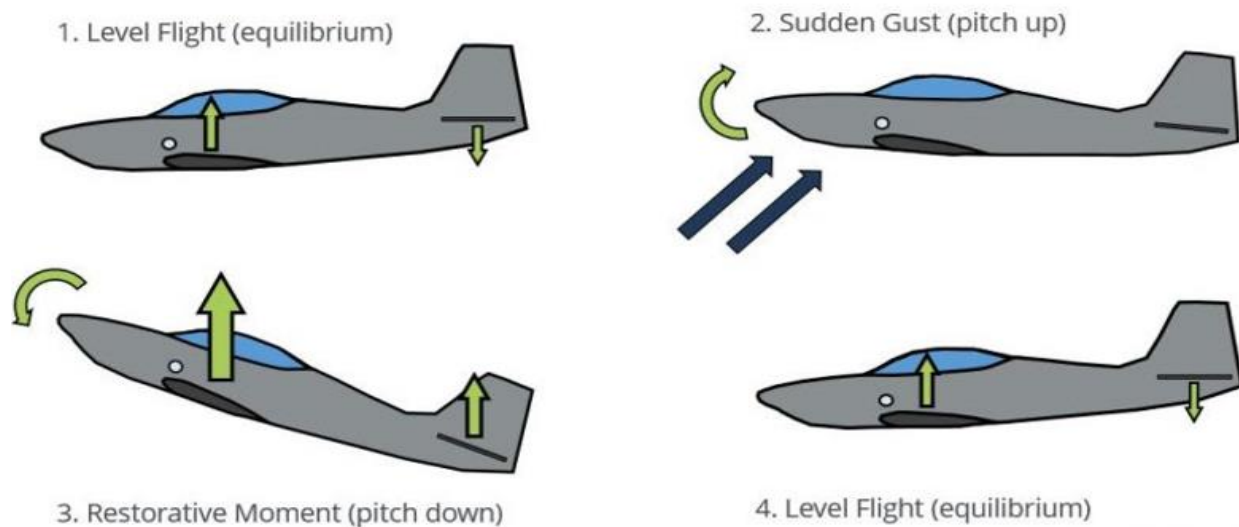


Figure II.6 Example of the response to an upward gust of an aircraft that is Longitudinal Statically Stable [19]

In order to balance this pitch-down moment generated by the wing in level flight, a moment of equal magnitude but opposite direction must be generated to keep the aircraft in balance. This moment is generated by the horizontal tail and is equal to the magnitude of the normal force generated by the stabilizer multiplied by the distance between the CG and the center of pressure (downforce) of the horizontal stabilizer. A conventional arrangement with the tail to the rear of the aircraft will necessitate that the aerodynamic force generated by the horizontal stabilizer be downward in level flight.

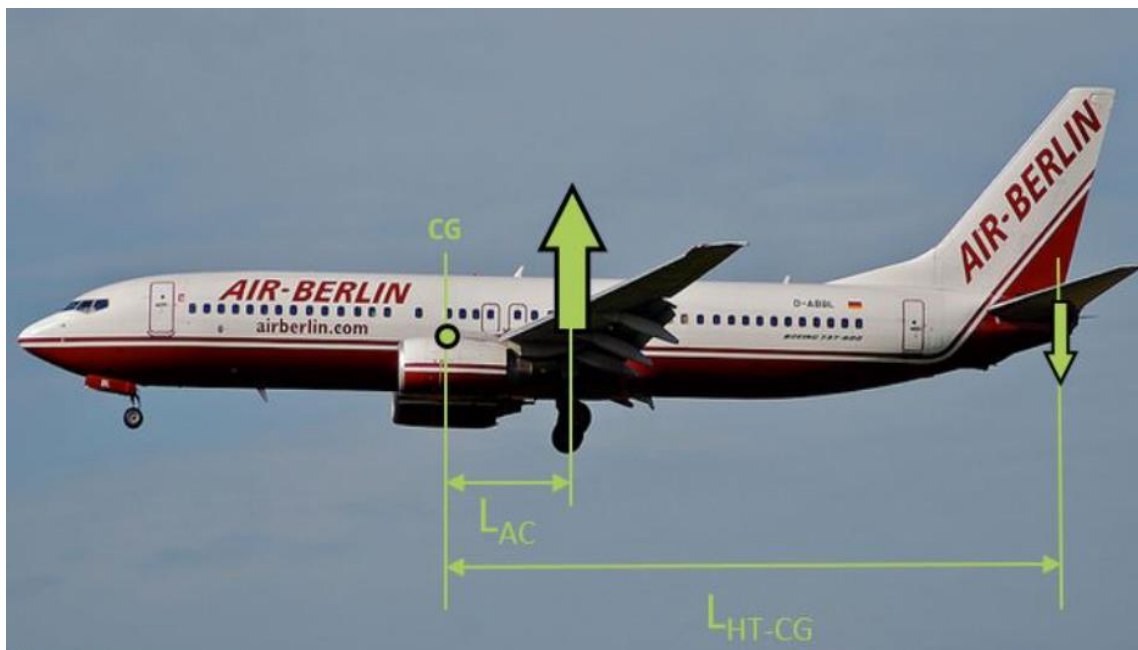


Figure II.7 Downward acting normal force on the horizontal stabilizer in a conventional arrangement [19]

Vertical Stabilizer

Like the way that the horizontal stabilizer controls the longitudinal stability of an aircraft, the vertical stabilizer is designed to control stability in the directional or yaw axis. Generally, the vertical stabilizer points upward and works in the same manner as the rear fin on a weathervane. An example of the contribution of the vertical stabilizer to yaw stability is shown below:

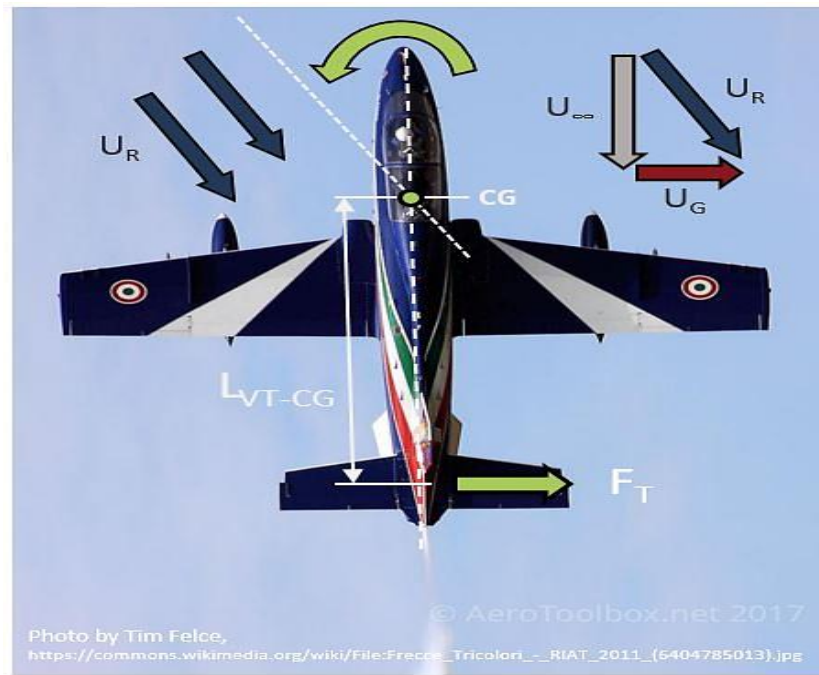


Figure II.8 Contribution of the vertical stabilizer to yaw (directional) stability [19]

Suppose an aircraft is flying and a gust of magnitude U_G hits the aircraft from the left-hand side. The gust causes the local velocity over the vertical tail to be such that the tail is effectively inclined at an angle of attack to the relative wind (U_R). This causes a lifting force (F_T) to be generated such that a moment $F_T \times L_{VT}$ will yaw the aircraft into the direction of the relative wind. This is a stable situation, much like a weathervane, the aircraft will always tend to point in the direction of the relative wind. If the vertical stabilizer was placed ahead of the center of gravity it would have a destabilizing effect and tend to push the aircraft away from the relative wind.

II.3.2 Sizing the Stabilizer Surfaces

Sizing the vertical and horizontal tail is an iterative process that during the preliminary stages of design, is largely empirical. A good starting point is to first study existing aircraft of similar size and configuration, and to use this as a basis for sizing your design. The primary design function of both stabilizing surfaces is to provide stability in their respective axes and so initially sizing surfaces according to what is currently flying should provide you with a good first approximation of the size required. Remember that the larger the final stabilizing surface, the greater that surface's contribution to the overall aircraft drag, and so the tail should be sized as small as possible but sufficiently large to ensure that all stability criteria are met.

One popular method in the preliminary sizing of stabilizing surfaces is to make use of non-dimensional volume ratios which relate the size of the wing and length of the aircraft to the required horizontal and vertical tail area. Remember to always use a consistent set of dimensions when calculating the ratios (m and m² or ft and ft²) [19].

Horizontal tail (stabilizer) volume ratio:

$$C_{HT} = \frac{S_{HT} \times L_{HT}}{A \times MAC}$$

From this equation we can determine the L_{HT} :

$$L_{HT} = \frac{MAC \times A \times C_{HT}}{S_{HT}} \dots\dots\dots (6)$$

Vertical tail (stabilizer) volume ratio:

$$C_{VT} = \frac{S_{VT} \times L_{VT}}{A \times b}$$

And from this one we can determine the L_{VT} :

$$L_{VT} = \frac{C_{VT} \times A \times b}{S_{VT}} \dots\dots\dots (7)$$

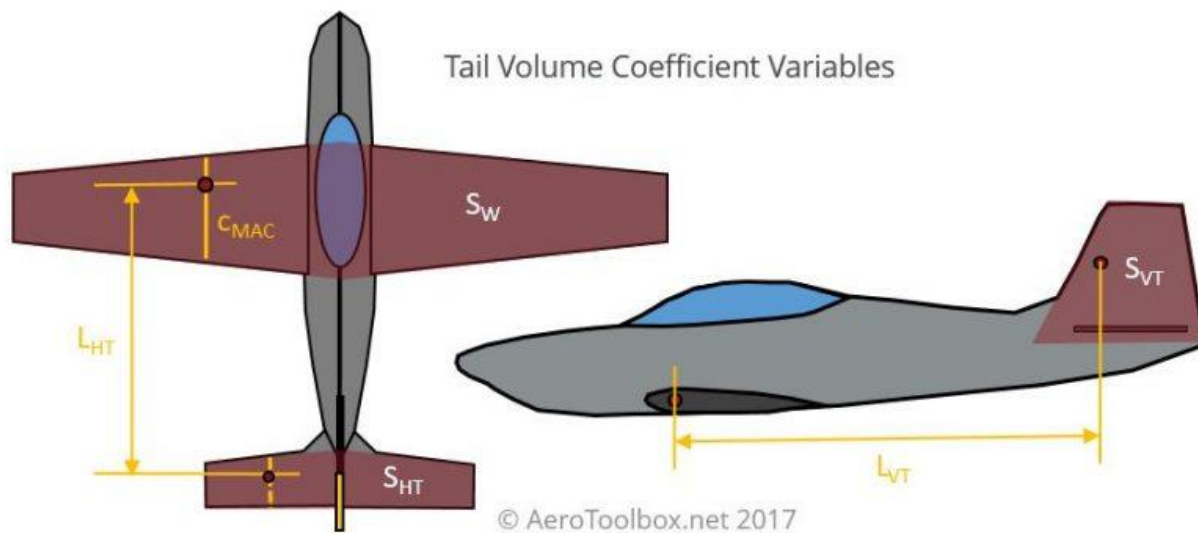


Figure II.9 Tail Volume Coefficient Variables [19].

Where:

A : Wing Area

MAC : wing Mean Aerodynamic Chord

b : wingspan

S_{HT} : Horizontal Tail Area

S_{VT} : Vertical Tail Area

L_{HT} : Length between the aerodynamic centers of the wing and horizontal tailplane

L_{VT} : Length between the aerodynamic centers of the wing and vertical tailplane

Different aircraft types have different target volume ratios, and some examples of aircraft types and corresponding target volume ratios are shown below [21].

Horizontal Tail Volume Coefficients:

Aircraft Type	Raymer	Roskam	Torenbeek	Howe	Schaufele	Jenkinson	Nicolai
Sailplane	0.500			0.500			
Civil props							
Homebuilts	0.500	0.467					
Personal					0.48-0.92		
GA ^a - Single engine	0.700	0.667		0.650			
GA ^a - Twin engine	0.800	0.786		0.850			
Commuter					0.46-1.07		
Regional Turboprop	0.900	1.075	1.006	1.000	0.83-1.47		
Jet							
Business Jets		0.721	0.691	0.700	0.51-0.99		
Jet transport	1.000	1.010	0.904	1.200	0.54-1.48	0.875	
Supersonic							
Cruise Airplanes		0.535					
Military							
Jet Trainer	0.700	0.639		0.650			
Jet Fighter	0.400	0.362			0.20-0.75		0.307
Military Transport	1.000	0.891	0.850	0.650			
Special Purpose							
Agricultural	0.500	0.526					
Flying Boat	0.700	0.641					

^a GA stands for General Aviation

Table II.1 List of Recommended Horizontal Stabilizer (tail) Volume Coefficient [21]

Vertical Tail Volume Coefficients:

Aircraft Type	Raymer	Roskam	Howe	Toren. ^a	Schaufele	Jenk. ^b	Nicolai
Sailplane	0.020		0.018				
Civil props							
Homebuilts	0.040	0.036					
Personal					0.024 ... 0.086		
GA- single engine	0.040	0.043	0.050				
GA- twin engine	0.070	0.062	0.065				
Commuter					0.041 ... 0.097		
Regional Turboprop	0.080	0.083	0.080	0.077	0.065 ... 0.121		
Jet							
Business Jets		0.073	0.065	0.069	0.061 ... 0.093		
Jet transport	0.090	0.079	0.090	0.074	0.038 ... 0.120	0.076	
Supersonic							
Cruise Airplanes		0.062	0.065				
Military							
Military Trainer	0.060	0.061	0.065				
Military Fighter	0.070	0.077			0.041 ... 0.130		0.064
Military Transport	0.080	0.073	0.065				
Special Purpose							
Agricultural	0.040	0.032					
Flying Boat	0.060	0.050					

^a Toren. stands for the author Torenbeek

^b Jenk. stands for the author Jenkinson

Table II.2 List of Recommended Vertical Stabilizer (tail) Volume Coefficients [21]

The following are some general rules of thumb that may prove useful when specifying the horizontal and vertical tail planform area [21]:

- A symmetrical airfoil profile should always be used for both the horizontal and vertical stabilizer as the net force acting on both will change direction during flight depending on which direction the elevator or rudder is deflected. Two common profiles to consider using are the NACA 0010 or NACA 0012 airfoil.
- The aspect ratio of the horizontal tail should always be less than the aspect ratio of the wing. Lower aspect ratio wings stall at higher angles of attack and so it follows that the horizontal stabilizer should have a lower aspect ratio so that control authority is still available after the wing has stalled.
- A typical aspect ratio for a vertical tail is in the range of 1.3 to 2.0 (here the aspect ratio is based on the span from root-to-tip as the span from tip-to-tip has no meaning in the case of a vertical stabilizer).
- The empirical method outlined above is useful as a first approximation as to the size and shape of the stabilizers required. This would typically form the input to a more detailed

analysis of the surfaces including sizing of the elevator, rudder, and associated trim tabs as well as a detailed study into the stability characteristics of the aircraft. Both a static and dynamic stability analysis would need to be undertaken and would include such calculations as:

- Longitudinal static stability (will the aircraft return to a neutral state after an upward or downward gust).
- Directional static stability (will the aircraft return to a neutral state after a crosswind gust).
- VMCA calculation (is the aircraft able to maintain directional control with one engine inoperative at a speed close to stall).
- Longitudinal and Lateral trim calculation (is the aircraft able to remain in trim for a variety of speeds and altitudes).
- Spin recovery
- Tail stall
- Deep stall
- Handling quality tests
- Horizontal stabilizer incidence

As you can see from the list of calculations given above there is a lot of analysis that goes into the sizing of the horizontal and vertical tail. What has been written above forms a basic introduction to the empennage surfaces present on an aircraft and should hopefully provide you with a starting point for how to go about the design of a tail for a new aircraft or drone.

Second part: Flight Dynamics

After highlighting some structural parameters and different calculation formulas in the first part. The design of a drone is not concluded until we dive in the most important part which is making it lift off from the ground i.e. take flight and keep it in the air in a stable and level flight.

To accomplish this, we are going to calculate the aerodynamic forces and moments acting on an aircraft in different flight conditions. These forces and moments depend on various factors, such as the aircraft geometry, the angle of attack, the airspeed, the altitude, and the control surface deflections. To perform these calculations, we need to know some basic concepts of aerodynamics, such as the lift and drag coefficients, the center of pressure, and the stability derivatives. We will also introduce some methods for estimating the aerodynamic coefficients from empirical data or computational simulations. The goal of this work is to provide a comprehensive and practical approach to the analysis of the flight parameters of an aircraft.

II.4 Theory of flight:

An aircraft has mass and is subjected to gravity; thus, it has weight. This weight acts vertically downward at the center of gravity. To get airborne an aircraft must produce an upward force to counteract the weight. We call this force lift. Lift is produced by airflow over the wings and is always measured normal to the relative airflow.

Aerodynamic drag is the force that resists motion through the air. Similar to how water impedes a swimmer, air impedes the motion of the aircraft. To overcome this drag requires a thrust force which is produced by an engine. There are therefore four fundamental forces acting on an aircraft: thrust and drag, lift and weight.

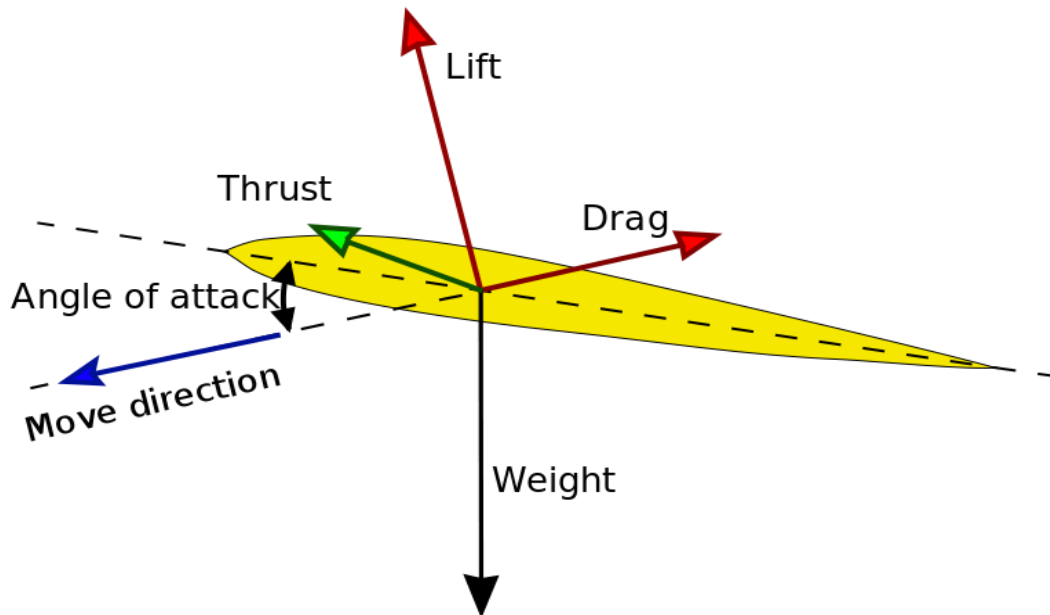


Figure II.10 The four aerodynamic forces applied on wing profile [22]

The wing profile (figure II.8) is the heart of the model. It therefore deserves some attention. The top of the profile is called extrados, the underside intrados. The line passing through the leading edge and the trailing edge is called the reference line. The chord is the segment of this line, going from the leading edge to the trailing edge. When air flows around a profile, pressure variations take place all around it.

The wing profiles are designed so that, in flight, a depression is created at the upper surface, while an excess pressure is established on the lower surface. This pressure difference causes a force pulling the profile both upwards and backwards, called "resultant".

This force applies at a particular point on the reference line: the center of pressure. The resultant can be decomposed into two different forces: the first, perpendicular to the direction of the flow, is the effective component: it is lift.

The second, parallel to the flow, is the inevitable component parasite. Its name: drag.

The values of these two forces for the entire wing are calculated by:

$$F_L = \frac{1}{2} \rho V^2 A C_L \dots\dots\dots (8)$$

$$F_D = \frac{1}{2} \rho V^2 A C_D \dots\dots\dots (9)$$

Where:

F_L : Lifting force (N)

C_L : Lifting coefficient

ρ : Density of fluid (kg/m³)

V : Flow velocity (m/s)

A : Wing Area (m²)

The coefficients C_L and C_D are a function of the angle of attack (or angle of incidence) of the profile, i.e. the angle that the reference line makes with the direction of flow. It is the way in which these coefficients vary with the angle of attack that determines the performance of a profile [17].

Since the wing area and the density of the air are assumed to be fixed, it is concluded that lift and drag vary in flight with two parameters: speed (squared) and angle of attack.

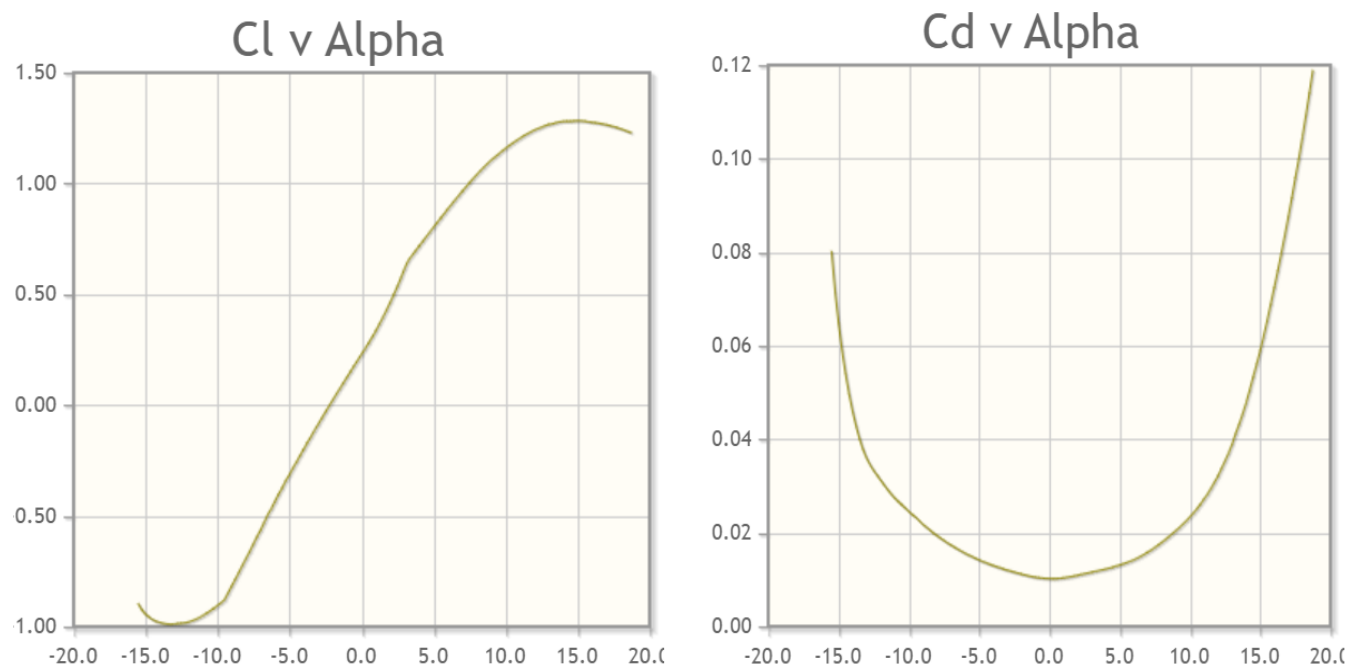


Figure II.11 The variation of C_D and C_L with the angle of attack [23].

Let us take a closer look at the variations of C_L and C_D as a function of the angle of attack (α): (Figure II.11) We can see that the curve representing C_L as a function of α is a straight line. For a certain value of α ("alpha zero", or zero lift angle), the C_L is zero, and therefore the lift is also zero. The C_L grows linearly with α , up to a maximum C_L value, beyond which the airfoil stalls, the angle of incidence being too great for the airflow around the airfoil to be even. C_D , on the other hand, is not a linear function of α . The curve is more like a parabola. Also, you may notice that, unlike C_L , C_D is never zero [17].

In other words, for the "alpha zero" incidence, the lift is zero, but the wing still drags. An angle of incidence corresponds to a value of C_L and a value of C_D . Fortunately for us, the value of C_D is on average almost a hundred times lower than that of C_L . The C_L / C_D ratio is also a factor that we will look at more closely later (Figure II.12). The two curves in figure II.11 can be combined into one by plotting the C_L as a function of the C_D for a given profile [17].

The resulting curve is called the drag polar curve of the profile. This representation is useful for comparing profiles with each other, but it is not sufficient in the context of a model design; This is because it does not provide any information on the angle of incidence. However, this type of information will be necessary in the rest of the method, especially when determining the correct angle of incidence of the wing.

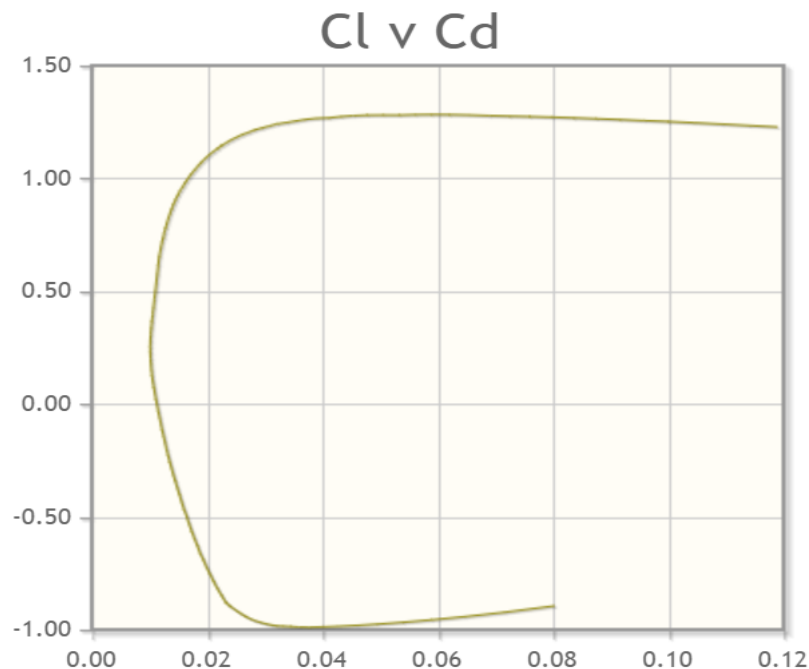


Figure II.12 Drag polar curve [23].

Let's go back to C_L and C_D : each profile has its polar, representing its performance for the entire range of angles of attack (extending approximately from -5° to 15°). In reality, it's more complex than that. Indeed, any profile works better the faster the flow, and the greater the chord of the profile.

A profile moving at 50 km/h in relation to the air will have a larger C_L and/or a smaller C_D than the same profile moving at 30 km/h with the same angle of attack. This is independent of the formulas of the forces given above; we are talking here about C_L and C_D , and not about lift or drag. In the same way, at the same speed, a profile is more effective if it is used with a longer chord. But then, how do you find your way around, if the polar of a profile is only valid for a chord value and a speed value? Fortunately, the effects of speed and chord on profile efficiency are quite similar. Doubling the speed has the same beneficial effect on performance as doubling the chord. We therefore use a very practical number, taking into account both the chord and the speed: Reynolds number [17].

The Reynolds number is defined as:

$$Re = \frac{\rho V L}{\mu} \dots\dots\dots (10)$$

where:

- ρ is the density of the fluid (SI units: kg/m^3)
- V is the flow speed (m/s)
- L is a characteristic length (m)
- μ is the dynamic viscosity of the fluid ($\text{Pa}\cdot\text{s}$ or $\text{N}\cdot\text{s/m}^2$ or $\text{kg}/(\text{m}\cdot\text{s})$)

The Reynolds number is representative of the conditions under which the profile works. Doing 10 cm of chord and flying at 40 km/h or doing 20 cm of chord and flying at 20 km/h, for a profile, it's the same. In both cases, the Reynolds number is 80,000. In agreement with what has been said above, it can be said that the profiles do not tolerate low Reynolds numbers, especially when they are hollow and/or thick.

In model aeronautics, the profiles work, depending on the model, at Re between 60,000 and 500,000 (or even 1,000,000 for models that are both very large and fast). C_L and C_D are therefore ultimately a function not only of the angle of attack, but also of the Reynolds number. Thus, a given profile has an infinity of polars, since there are an infinite number of Reynolds ... In fact, we are content to have the polars corresponding to a few Re (often 100,000, 200,000 and 500,000).

To calculate the performance, it will be sufficient to choose the Re that is closest to the flight conditions of the future model. (Figure II.13) shows a typical set of polars of the same profile, for five different Re s. We see that the drag (C_d) increases when the Re decreases, with the polars moving further and further to the right on the graph. As for the C_L max, it decreases with the low Re Number [17].

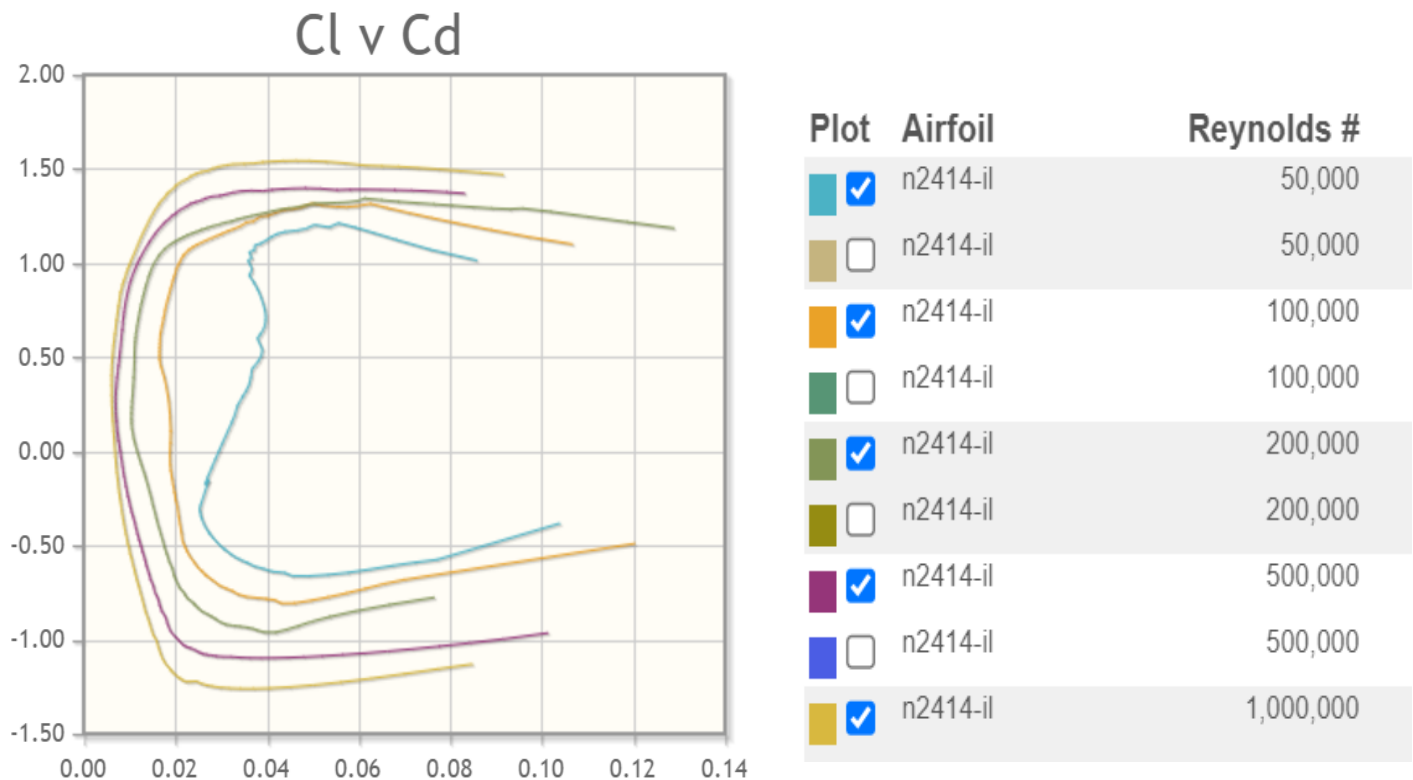


Figure II.13 Variation of drag polar curves with different Reynolds numbers [23].

II.5. Steady flight:

In steady flight, the sum of these opposing forces is always zero. There can be no unbalanced forces in steady, straight flight based upon Newton's Third Law, which states that for every action or force there is an equal, but opposite, reaction or force. This is true whether flying level or when climbing or descending. It does not mean the four forces are equal. It means the opposing forces are equal to, and thereby cancel, the effects of each other. In Figure II.14, the force vectors of thrust, drag, lift, and weight appear to be equal in value. The usual explanation states (without stipulating that thrust and drag do not equal weight and lift) that thrust equals drag and lift equals weight. Although true, this statement can be misleading. It should be understood that in straight, level, unaccelerated flight, it is true that the opposing lift/weight forces are equal. They are also greater than the opposing forces of thrust/drag that are equal only to each other. Therefore, in steady flight:

- The sum of all upward components of forces (not just lift) equals the sum of all downward components of forces (not just weight)
- The sum of all forward components of forces (not just thrust) equals the sum of all backward components of forces (not just drag)

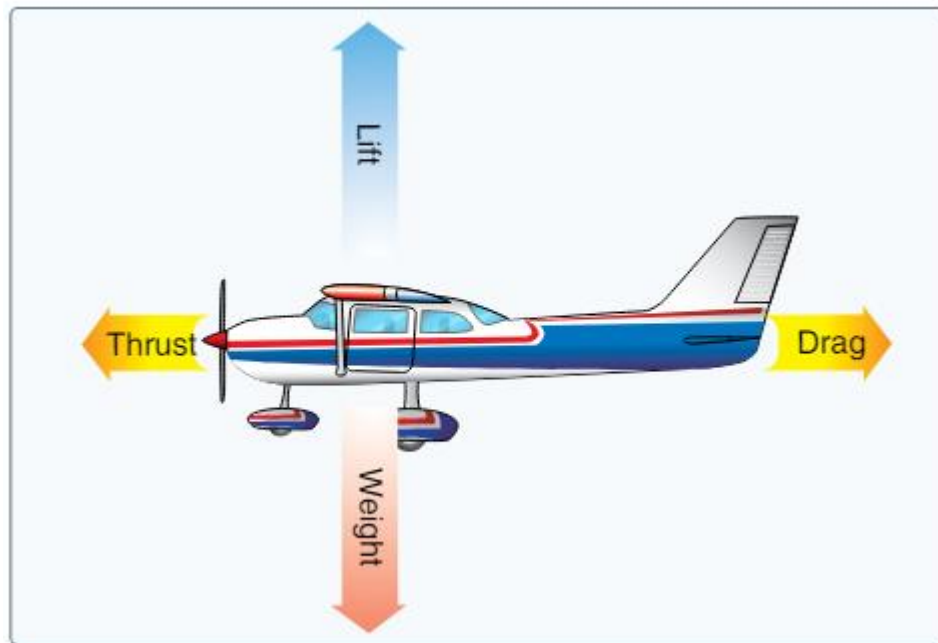


Figure II.14 The four aerodynamic forces acting on an aircraft [24].

This refinement of the old “thrust equals drag; lift equals weight” formula explains that a portion of thrust is directed upward in climbs and slow flight and acts as if it were lift while a portion of weight is directed backward opposite to the direction of flight and acts as if it were drag. In slow flight thrust has an upward component. But because the aircraft is in level flight, weight does not contribute to drag (FigureII.15) [24].

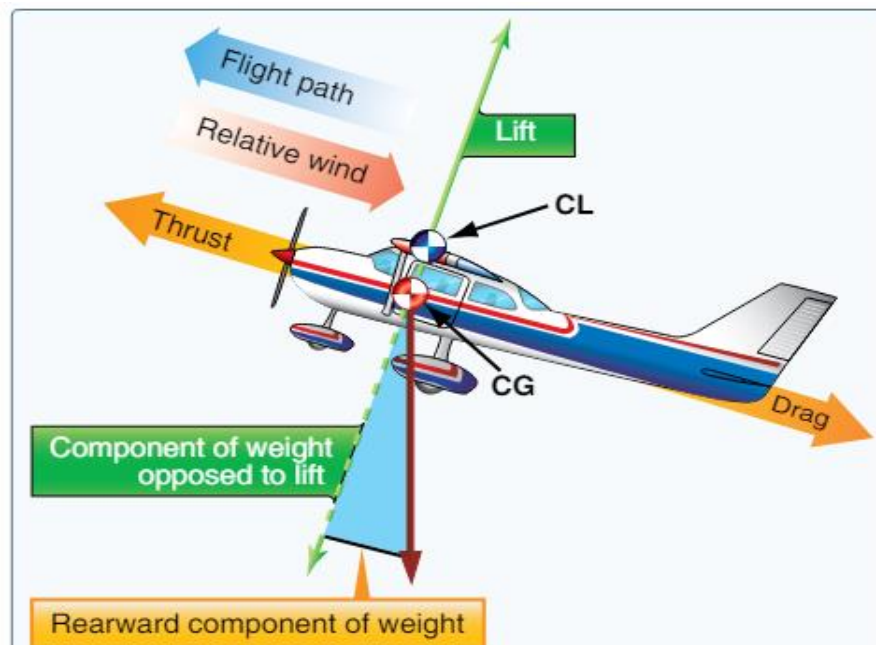


Figure II.15 Force vectors during a stabilized climb [24].

Mathematically it translates to:

$$L = \frac{1}{2} \rho V^2 S C_L$$

$$D = \frac{1}{2} \rho V^2 S C_D$$

Where:

L: Lift force (N)

D: Drag force (N)

ρ : The density of the fluid (kg/m³)

V: The flow speed (m/s)

S: Wing Area (m²)

C_L , C_D : lift and drag coefficient

On the other hand, we have equilibrium on the vertical axes:

$$W = M \times g \dots\dots\dots (11)$$

Where:

M: mass of the drone or plane (kg)

g: force of gravity (m/s²)

When the center of gravity and center of pressure are co-located, the speed remains constant, a balance has been reached. The direction of flight makes a certain angle with the horizontal axes called: Glide slope which is a measure of the efficiency of flight, often expressed in terms of horizontal distance traveled relative to the vertical distance. For example, if an aircraft travels 60 kilometers horizontally for every kilometer it descends, it will have a glide slope of 60:1. This is directly related to the Lift-to-Drag ratio (L/D ratio). An aircraft with a high L/D ratio will have a higher glide slope, meaning it can fly further for each unit of height it loses. This is why gliders, which have very high L/D ratios, can fly long distances even without an engine.

This ratio is an indication of the aerodynamic efficiency of an airplane. An airplane has a high L/D ratio if it produces a large amount of lift or a small amount of drag [25].

The lift coefficient (C_L) and drag coefficient (C_D) are defined as follows:

- Lift Coefficient (C_L):

$$C_L = \frac{L}{q \times A}$$

- Drag Coefficient (C_D):

$$C_D = \frac{D}{q \times A}$$

$$\text{Where: } q = \frac{1}{2} \rho V^2$$

Therefore, the Lift-to-Drag ratio can be expressed as the ratio of these coefficients:

$$L/D = \frac{F_L}{F_D} = \frac{C_L}{C_D} \dots\dots\dots (12)$$

Lift to drag ratio is given by the ratio of the glider's lift and drag coefficients. In a way, it represents the performance of the model. The speed on the trajectory can also be calculated as a function of C_L and C_D ; it is sufficient to rewrite the balance of forces by replacing the glide slope angle by tangent arc of C_D/C_L . After simplification, we obtain [17]:

$$V_T = \sqrt{\frac{2Mg}{\rho A}} \times \sqrt{\frac{1}{C_L^2 + C_D^2}} \dots\dots\dots (13)$$

Where:

V_T : Trajectory speed (m/s)

M: Masse (kg)

g: Gravity force (9,81 m/s²)

ρ : Density (1,225 kg/m³)

A: Wing Area (m²)

C_L , C_X : Lift and Drag coefficient (without a unit)

The horizontal speed and the sink rate are then obtained by using [17]:

$$V_H = V_T \times \cos(\arctan(\frac{C_D}{C_L})) = V_T \times \frac{C_L}{\sqrt{C_L^2 + C_D^2}} \dots\dots\dots (14)$$

V_H : Horizontal Speed (m/s)

V_T : Vertical Speed (m/s)

We have just seen what the balance of forces entails during gliding. These performance calculations, made from the C_L and C_D values of the complete glider, will allow you to choose the angle of incidence of the wing profile that best corresponds to what you want to achieve as a standard flight. The second condition for the glider to maintain its trajectory lies in the equilibrium of moments at the center of gravity (CG), as mentioned above. Two forces are likely to have a moment with respect to the CG: the lift of the wing, and the lift of the stab. In order for equilibrium to take place, it is therefore necessary to have [17]:

$$M_{LW} + M_{LS} = 0$$

M_{LW} : moment of lift generated by the wing in relation to the CG (Newton meter Nm).

M_{LS} : moment of lift generated by the stabilizer in relation to the CG (Newton meter Nm).

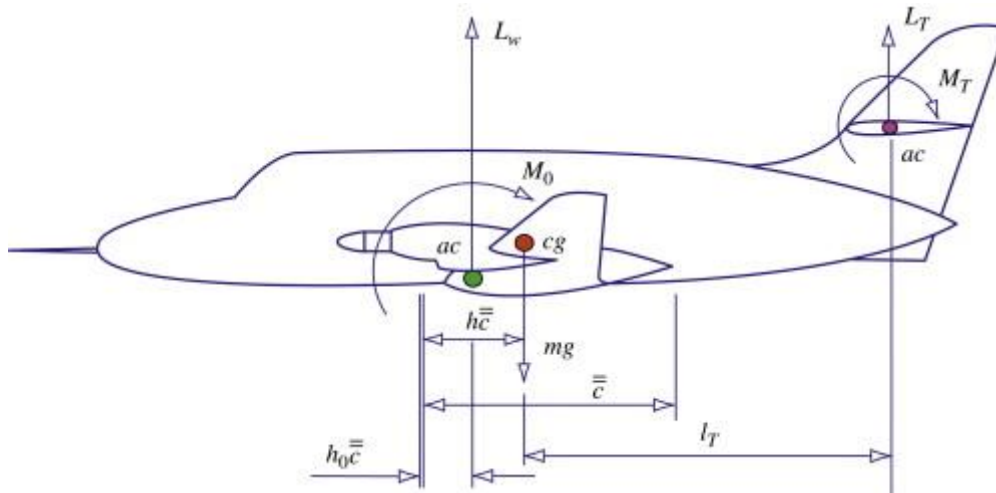


Figure II.16 pitching moment model on CG and center of pressure [26]

Figure II.16 shows a situation where this is verified. We can have fun developing this equation (we end up with a relationship linking distance CP-CG and C_L of stab). The easiest way to solve it is to check:

$$ML_w = 0$$

$$ML_s = 0$$

The moment of a force with respect to a point is zero in various cases, including the following two:

- The force is zero.
- The distance between its point of application and the reference point is zero.

In this case, we will use one of each: for the stabilizer, we will make the lift zero, and for the wing, we will make the distance from the center of thrust to the center of gravity zero (CP and CG will be collocated). The model will have to be balanced exactly at the center of pressure, and its stabilizer adjusted so that it does not produce any lift in normal flight. Note that this simple solution is also the most efficient: in fact, the stabilizer will have the least drag when it has zero lift [17].

II.5.1 Pitch axis centering and stability:

We started to see how to adjust the glider according to a desired flight balance. A glider in equilibrium does not mean a stable glider in any way. Let us not confuse; "Equilibrium" means constant speed, in value and direction. "Stability" means return to the equilibrium position if one has been removed from it. We even separate stability into two: static stability, and dynamic stability.

An object is said to be statically stable if, when it is moved a little away from its equilibrium position, the forces and moments at work tend to bring the object back to its starting position. Dynamic stability, on the other hand, describes the way in which the return to equilibrium takes place over time, for example by studying the trajectory of the object. The stability of your model

on the pitch axis is ensured by the stabilizer. The static stability rate is therefore a function of the stabilizer volume. Specifically, here is how it looks: there's a point on the longitudinal axis of the model called the Aft Center of Gravity Limit (ACGL).

The static stability of the model is guaranteed if you center it in front of this limit. The position of this point on the MAC is calculated as follows [17]:

$$ACGL = MAC \times (0.25 + V_s \times \frac{AR+2}{AR} \times \frac{AR_s}{AR_s+2}) \dots\dots\dots (15)$$

ACGL: Aft Center of Gravity Limit

MAC: mean aerodynamic chord

Vs: stabilizer volume coefficient

AR: wing's aspect ratio

ARs: stabilizer aspect ratio

To determine the ACGL you must choose an important parameter: the "stabilizer volume", indicated by Vs. A sufficient value of Vs ensures the stability of the model on the pitch axis. This should be between 0.4 and 0.8. Here are some clues to choose the right Vs:

The rotational inertia of a glider around its pitch axis is comparatively much lower than that of an airplane. This means that the current values of Vs for a glider are around 0.5, while those for an aircraft are more often close to 0.6 or 0.7.

The slower your model is designed to fly, the greater its Vs will have to be. Conversely, if you are designing a speed model, a low Vs will be enough [17].

II.6 Conclusion:

In conclusion, the chapter on airplane and drone design has provided a comprehensive overview of the mathematical equations and formulas that underpin these fields. We have delved into the principles of aerodynamics, exploring key concepts such as the Lift-to-Drag ratio, Center of Pressure, and Center of Gravity. We have seen how these factors influence an aircraft's stability and control, and how they are crucial in determining the efficiency of flight.

We have also examined the importance of the Mean Aerodynamic Chord (MAC) and the role it plays in determining the position of the Center of Gravity. Furthermore, we've learned about the Aft Center of Gravity Limit (ACGL), a critical parameter in aircraft design that ensures safe and stable flight.

In the context of drones, these principles take on additional layers of complexity due to their unique design and operational requirements. Drones often need to operate in more varied and challenging conditions than traditional aircraft, making the understanding and application of these mathematical principles even more crucial.

From the intricate calculations of aerodynamic forces to the careful balancing of weight and lift, this chapter has underscored the importance of mathematics in aircraft and drone design. As we move forward, these foundational concepts will continue to guide us in the pursuit of more efficient, stable, and capable flying machines.

In essence, the science of flight is a testament to the power of mathematical modeling and analysis. Whether we are designing a jumbo jet or a compact drone, the same fundamental principles apply. It is a fascinating field that continues to evolve, driven by ongoing advancements in technology and our ever-deepening understanding of the physics of flight. As we close this chapter, we look forward to exploring new frontiers in the next chapters.

Chapter III

***Presentation of the model studied
and the calculation of its various
parameters***

III.1 Introduction

This chapter embarks on an in-depth exploration of aircraft design, with a specific focus on Unmanned Aerial Vehicles (UAVs), commonly known as drones. The study is grounded in the principles of aerodynamics and the mathematical equations that govern these principles mentioned in the previous chapter.

The initial phase of the study involves the identification of the specific type of UAV under consideration. This is a critical step as it sets the foundation for all subsequent calculations and design considerations. The type of aircraft, whether it's a fixed-wing drone, a quadcopter, or a more complex multirotor design, presents unique challenges and opportunities that significantly influence the design process.

Following the identification of the aircraft type, the study delves into the complexities of its design. This involves the calculation of various values and relationships that shape the drone and determine its flight characteristics. Key parameters such as the weight of the aircraft, the length of the wing, and the aerodynamic chord are calculated and analyzed. Each of these factors plays a pivotal role in the aircraft's flight characteristics, influencing its speed, maneuverability, stability, and fuel efficiency.

In addition to these primary design elements, the study also explores the role of secondary structures such as the stabilizer. While these components may seem less significant, they can have a substantial impact on an aircraft's performance. By understanding their function and learning how to optimize their design, we can enhance the overall performance of our aircraft.

The study also delves into the mathematical equations and formulas that underpin these design considerations. From the basic principles of lift, drag, and thrust to the complex calculations of aerodynamic forces, the study unravels the mathematical underpinnings that make flight possible.

In essence, this chapter is more than just a study of aircraft design. It's a deep dive into the science of flight, a journey of discovery that will equip us with the knowledge and skills to design efficient, effective, and innovative drones. So, buckle up and get ready for takeoff as we set out on this exciting adventure into the world of drone design.

III.2 SKYEYE SIERRA UAV

Performance, ease of use and high autonomy - the ElevonX SkyEye UAS is a product based around the concept of modularity. The smart modular UAS solution allows the user to have a competitive edge of UAS services by providing them with a tool that can switch between different types of tasks with minimal changes on the UAV platform, from multispectral mapping to surveillance missions in a matter of minutes. The core of our modular system is the SkyEye payload module, which was designed to house different types of payloads (from multispectral cameras to retractable surveillance gimbals). This high-end glass fibre-kevlar composite module's main features are: Large cargo bay (10 liters of volume, max dimensions 60x18x14 cm) Easy cargo access (top and bottom hatch, bottom hatch 25x16 cm) Integrated cargo rail with predefined fixpoints Modular propulsion options (gas/electric pusher or electric tractor)) Removable fix-points for catapult launch Optional landing gear (requires smooth take-off and landing surface) Removable nose cone (optional transparent nose cone for forward looking

camera installation) Streamlined design with highly visible livery (optional custom design)
Wing integrated avionics and parachute bay, payload bay dedicated for payload only [27].



Figure III.1 The ElevonX SKYEYE DRONE [27]

III.2.1 Technical details:

Domain	industrial
Applications	surveillance
Type	Fixed wing
Engine type	electric or gas motor
Maximum load	5 Kg
Autonomy	270 min, 480 min
Mass	12.5 Kg
Airspeed (cruise)	18 m/s (65 km/h)
Airspeed (max)	35 m/s (125 km/h)

Table III.1: Technical details of the SKYEYE SIERRA [27]

III.3 Structure (first part of the design process)

The following structural parameters of the SKYEYE SIERRA drone are calculated based on the technical details given in Table III.1 and some assumptions:

III.3.1 Wing area

The wing area of an aircraft or glider is the area of the wings projected on the horizontal plane (visible in the top view).
It is calculated like any other area in mathematics. The area connecting the wings through the fuselage is included in the calculation [28].

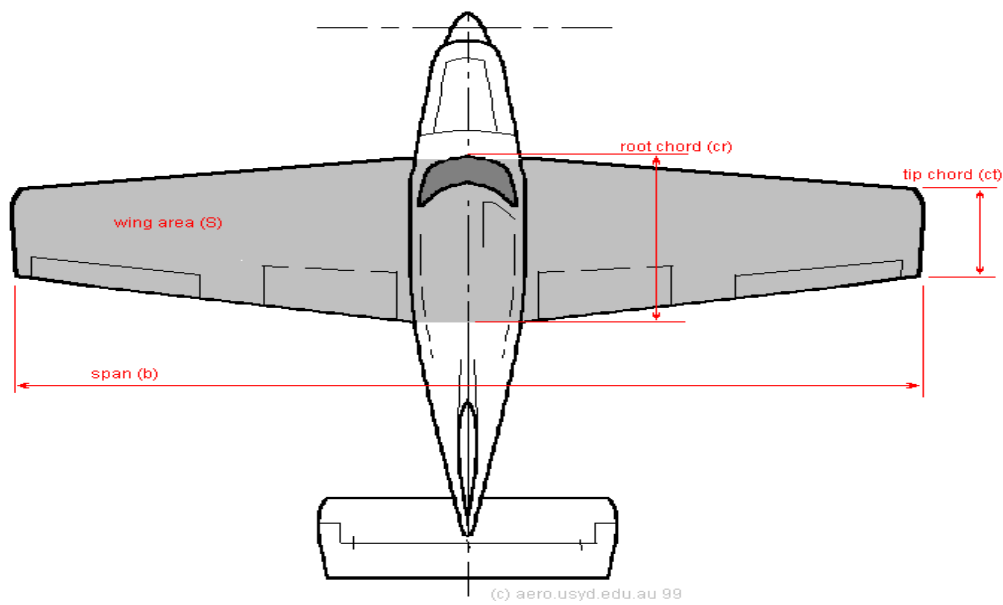


Figure III.2 Trapezoidal wing area [28]

$$A = b \times \frac{(Cr+Ct)}{2} \dots\dots\dots (1)$$

As we saw in chapter II, the wing area is calculated using the formula number (1).

We have the wingspan and both wing chords, let’s start the math:

With: A: wing area (m²) (designated by ‘S’ in figure III.2)

B: 3.096 (m)

Cr: 0.36 (m)

Ct: 0.235 (m)

$$A = 3.096 \times \frac{(0.36+0.235)}{2}$$
$$A= 0.921 \text{ (m}^2\text{)}$$

III.3.2 Aspect ratio

The aspect ratio of a trapezoidal wing is the ratio of its span to its mean chord. It shows how stretched out or flattened the wing is. The aspect ratio can affect the performance of drone wings, as it influences the lift, drag, and stability.

The aspect ratio is dimensionless, so it does not depend on the units of measurement.

To calculate the aspect ratio of a trapezoidal wing, we divide its span by its mean chord. As shown on the formula number (2):

$$AR = \frac{b^2}{A} \dots\dots\dots (2)$$

b= 3.096 (m)

A= 0.921 (m²)

$$AR=\frac{3.096^2}{0.921}$$

AR= 10.407 (without a unit)

III.3.3 Wing loading

The drone identified earlier, SKYEYE SIERRA, has an empty weight of 12.5 kg and can take up to 5k kg of payload, this payload differs from cameras to different electronic equipment depending on the mission and the intended use of the SKYEYE SIERRA, this mass will play an important roll in our work, from it will try to create different drone’s designs and sizes by changing the mass.

For now, and in the current module we are working on, will use the total mass of 17.5 kg (12,5+ 5kg payload).

We have our mass, and we calculated the wing area using equation (1), we can determine the wing loading using [17]:

$$n = \frac{M}{A} \dots\dots\dots (3)$$

n: Wing loading (kg/m²)

M: Dorne total mass (kg) = 17,5 (kg)

A: Wing area (m²) = 0.921 (m²)

$$n = \frac{17,5}{0.921}$$

n = 19 (kg/m²)

III.3.4 Mean Aerodynamic Chord (MAC)

In the UAV studied, we have a trapezoidal wing shape, which makes the calculation of its mean aerodynamic chord a little complicated, for that we will use the formula giving earlier in chapter II [17]:

$$MAC = \frac{2}{3} \times \frac{Cr^2+Cr\times Ct+Ct^2}{Cr+Ct} \dots\dots\dots (4)$$

With:

Cr: Chord root 0.36 (m)

Ct: Chord tip 0.235 (m)

$$MAC = \frac{2}{3} \times \frac{0.36^2+0.36\times 0,235+0.235^2}{0.36+0.235}$$

MAC = 0.301 (m)

III.3.5 Mean Aerodynamic Chord location

It is not only enough to calculate the mean aerodynamic chord in UAVs design, we also have to determine its location on the wing in order to determine the CG (center of gravity) location on the Mean Aerodynamic Chord, this plays an important part in the study of airplanes design and wing performance.

When we look at the location of the MAC equation (5) in chapter II:

$$D=\frac{1}{3}\times\frac{(Cr+2Ct)}{(Cr+Ct)}\times f\text{ (5)}$$

we notice that we need to have the sweep back angle (*f*) of the wing tip in order to calculate this location, unfortunately this information is not available to our knowledge.

Instead, we will jump to another method, locating the MAC by graphic drawing [29].

Measure the root and tip chord then draw the following lines on the plans:

At the root of the wing, draw a line parallel to the centerline of the fuselage extending forward from the leading edge and rearward from the trailing edge. Both lines should be the length of the tip chord.

Do the same thing at the tip but draw the lines the length of the root chord.

Connect the ends of the lines so that they create an "X" over the wing panel. Where the two lines intersect is the spanwise location of the Mean Aerodynamic Chord [29].

It will be simpler when visualized as in figure III.3.

As the location of the Mean Aerodynamic Chord is not determined mathematically, we will not be using this equation or formula in our MATLAB program to determine different drones designs and parameters using a different mass.

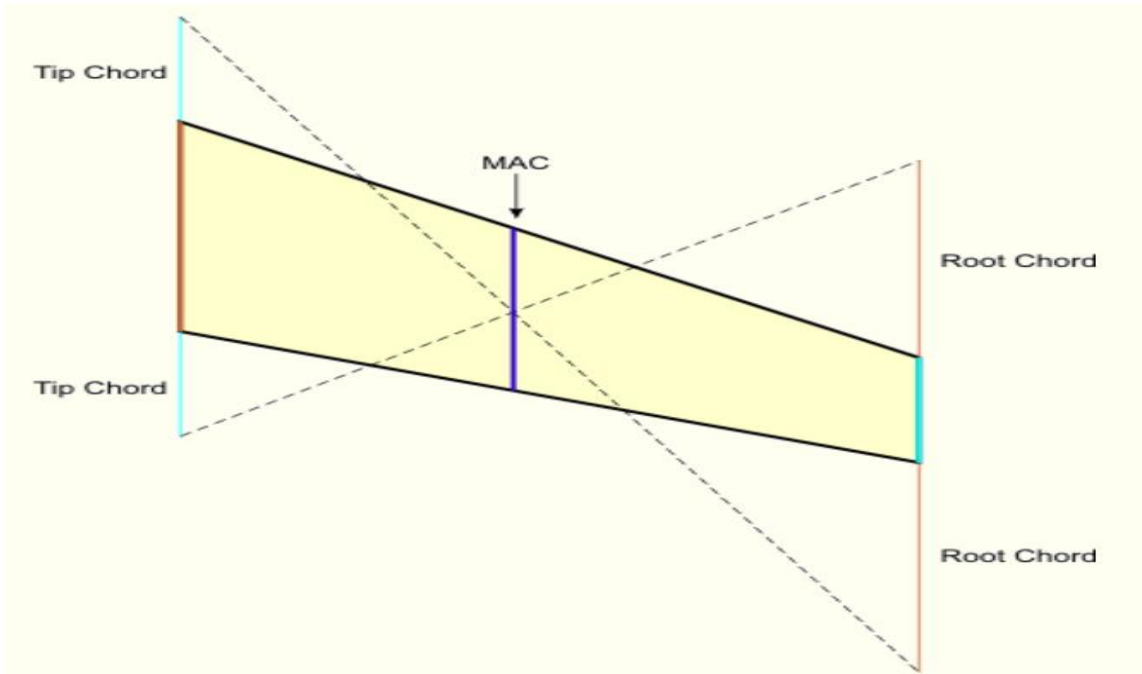


Figure III.3 Locating the Mean Aerodynamic Chord using the drawing method [29]

III.3.6 Aircraft stabilizer

Now that we have examined the drone’s wing parameters and equations. We will proceed to another crucial element of the drone's design, which is the aircraft tail or formally called the stabilizer.

III.3.6.1 Length between the aerodynamic centers of the wing and horizontal tailplane

Start by drawing your stabilizer in a corner of the sheet; it is not yet known how far to place it from the wing. Its surface area (S_s) will be between 10 and 20% of the wing area, as for the wing. Now you have to choose an important parameter: the "stab volume", denoted C_{HT} (Horizontal tail volume ratio) and C_{VT} (Vertical tail volume ratio). A sufficient value of these coefficients ensures the stability of the model on the pitch and roll axis. This should be between 0.4 and 0.8. Here are some clues to choose the right coefficient: The rotational inertia of a glider around its pitch axis is comparatively much lower than that of an airplane. This means that the current values of C_{HT} for a glider are around 0.5, while those for an aircraft are more often close to 0.6 or 0.7. The slower your model is designed to fly, the greater its C_{HT} will have to be. Conversely, if you are designing a speed model, a low C_{HT} will suffice [17]. For the values of C_{HT} and C_{VT} we will go back to Table II.1 and Table II.2. From Table II.1 we chose the homebuilt civil props coefficient because that being the closest aircraft type to our module. Taking the Raymer for example: $C_{HT} = 0.5$

$$C_{HT} = \frac{S_{HT} \times L_{HT}}{A \times MAC} \quad [21]$$

From this C_{HT} equation we can determine the L_{HT} :

$$L_{HT} = \frac{MAC \times A \times C_{HT}}{S_{HT}} \quad \dots\dots\dots (6)$$

Before we calculate the L_{HT} we have to determine the horizontal tail area S_{HT} . As mentioned earlier, it should be equal to around 20% of the wing area.

$S_{HT} = 0.2 \times A \quad \rightarrow \quad S_{HT} = 0.2 \times 0.921$
 $S_{HT} = 0.184 \text{ (m}^2\text{)}$

We have:

L_{HT} : Length between the aerodynamic centers of the wing and horizontal tailplane

MAC: Mean Aerodynamic Chord= 0.301 (m)

A: Wing area = 0.921 (m²)

C_{HT} : Horizontal tail volume coefficient = 0.5 (without a unit)

S_{HT} : Horizontal tail area = 0.184 (m²)

$$L_{HT} = \frac{0.301 \times 0.921 \times 0.5}{0.184}$$

$L_{HT} = 0.753 \text{ (m)}$

III.3.6.2 Length between the aerodynamic centers of the wing and vertical tailplane

Vertical tail (stabilizer) volume ratio:

$$C_{VT} = \frac{S_{VT} \times L_{VT}}{A \times b} \quad [21]$$

And from the equation above we can determine the L_{VT} :

$$L_{VT} = \frac{C_{VT} \times A \times b}{S_{VT}} \quad \dots\dots\dots (7)$$

Where:

L_{VT} : Length between the aerodynamic centers of the wing and vertical tailplane

b: Wingspan = 3.096 (m)

A: Wing area = 0.921 (m²)

C_{VT} : Vertical tail volume coefficient = 0.04 (without a unit) (value taking from table II.2)

S_{VT} : Vertical tail area = 0.184 (m²)

Before we calculate the L_{VT} , we need to mention that our module, as shown in Figure III.1, has an inverted V stabilizer. This means that this particular tail surface serves as both a horizontal and vertical surface simultaneously. That means that $S_{HT} = S_{VT}$ [21].

$$L_{VT} = \frac{0.04 \times 0.921 \times 3.096}{0.184}$$

$L_{VT} = 0.619 \text{ (m)}$

We will be resuming the first part of chapter III in the tables below:

Data	Value
Mass (M)	17.5 kg
Wingspan (b)	3.096 m
Root Chord (Cr)	0.36 m
Tip Chord (Ct)	0.235 m
SHT=0.2*A	0.184 m2
SVT= 0.2*A	0.184 m2
CHT	0.5
CVT	0.04

Table III.2 Giving data for the calculation of the structural parameters

Calculated parameters	Value
Wing area	0.921 m ²
Aspect ratio	10.407 (no unit)
Wing loading	19 kg/m ²
MAC	0.301 m
L _{HT}	0.753 m
L _{VT}	0.619 m

Table III.3 Calculated structural parameters

III.4 Flight Dynamics (second part of the design process)

In this part of the design process, we will dive into the different performance parameters and calculate their values. We will consider the following aspects of flight dynamics: stability and control, take-off and landing, climb and cruise, and maneuverability. For each aspect, we will use the data obtained from the previous steps, such as the dimensions, weights and different structural parameters of the aircraft, and apply the relevant equations and models to estimate the performance of the aircraft.

By the end of this part, we will have a comprehensive understanding of how the aircraft behaves in different flight conditions and scenarios.

III.4.1 Lift and Drag

Lift and drag are the two main aerodynamic forces acting on an aircraft. Lift is the force that opposes the weight of the aircraft and keeps it in the air. Drag is the force that opposes the forward motion of the aircraft and reduces its speed. The ratio of lift to drag is called the aerodynamic efficiency and determines how well the aircraft can perform in different flight regimes.

In chapter II, we discussed how to estimate the lift and drag coefficients of the aircraft based on its geometry, airfoil characteristics, angle of attack and Reynolds number. We also learned how to use the polar curve to find the optimal angle of attack for maximum lift or minimum drag. In this section, we will use these coefficients to calculate the actual lift and drag forces experienced by the aircraft at various speeds and altitudes. We will also analyze how the lift and drag vary with different flight parameters, such as the density, viscosity and pressure of the air. This will help us understand the limitations and trade-offs involved in designing an efficient aircraft. In this work we are limited to fixed values of density and speed values to simplify the calculation and to keep it all under the method we based our work on: SPP (Simple, practical and Performant).

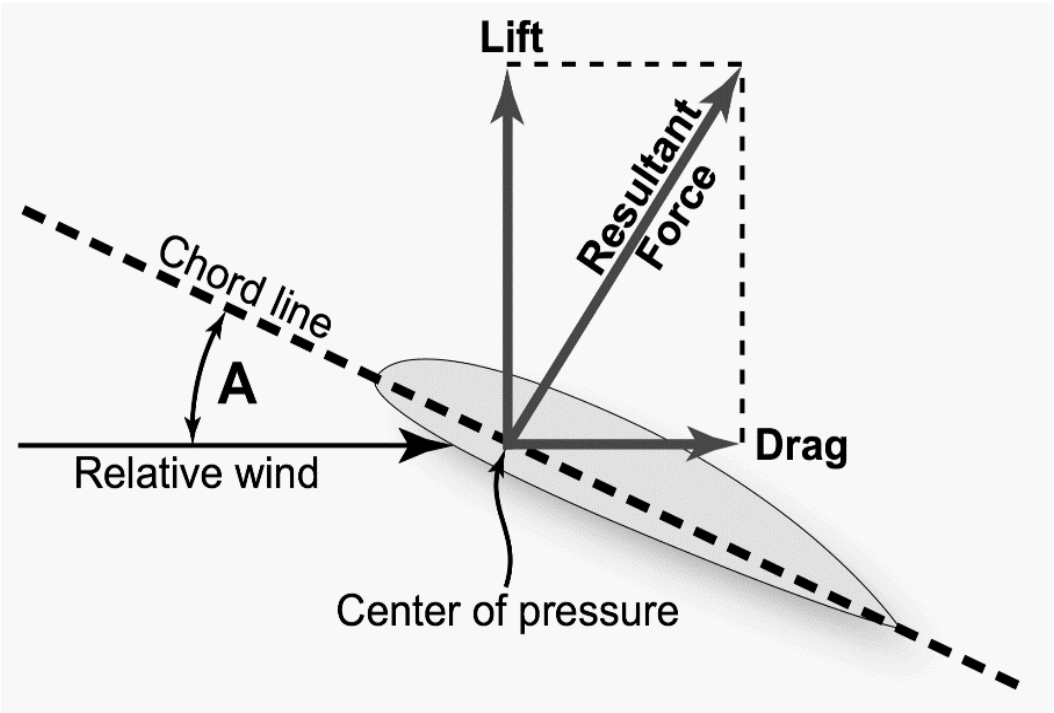


Figure III.4 Lift and Drag aerodynamic forces on a wing profile [30]

In order to compute the actual magnitude of the lift and drag forces acting on the aircraft, we need to multiply the coefficients obtained in the previous chapter by some factors that depend on the physical properties of the air and the flight conditions. These factors include the air density, the dynamic pressure, and the reference area of the wing. The formulas for calculating the lift and drag forces are given by equations (8) and (9), respectively, where ρ is the air density, v is the true airspeed, A is the wing area, C_L is the lift coefficient, and C_D is the drag coefficient. By using these formulas, we can estimate the amount of force required to sustain the aircraft in level flight or to overcome the aerodynamic resistance. In addition, we can also examine how the lift and drag forces change with respect to different variables (we will be using fixed values for our work), such as the airspeed, the altitude, the angle of attack, and the aircraft configuration. This will enable us to evaluate the performance and efficiency of the aircraft under various scenarios and constraints.

$$F_L = \frac{1}{2} \rho V^2 A C_L \dots\dots\dots (8)$$

$$F_D = \frac{1}{2} \rho V^2 A C_D \dots\dots\dots (9)$$

F_L : Lift force (N)

F_D : Drag force (N)

ρ : Air density = 1.225 (kg/m³)

V : Air flow velocity = 35 (m/s)

C_L: Coefficient of Lift

C_D: Coefficient of Drag

In order to calculate the maximum lift generated by our module, we will be using the maximum airspeed giving in the technical details of the SKYEYE SIERRA in Table III.1 (35 m/s)

The Lift and Drag forces will vary with the change in speed and in angle of attack, after using the maximum airspeed to calculate both forces, we must set a specific AOA to work on.

A website is available online to all aeromodellers and aviation enthusiasts for free, it is called “<http://airfoiltools.com>” on its website you can choose any wing profile and it will automatically generate the Lift according to the AOA in and the Drag according to the AOA in Figure II.11, in addition to the Drag polar curve as illustrated in Figure II.12 [23].

From figure II.11 with an angle of attack of 5°:

$$C_L = 0,79$$

$$C_D = 0.015$$

$$F_L = \frac{1}{2} \times 1.225 \times 35^2 \times 0.921 \times 0.79$$
$$F_L = 545.92 \text{ (N)}$$

and

$$F_D = \frac{1}{2} \times 1.225 \times 35^2 \times 0.921 \times 0.015$$
$$F_D = 10.36 \text{ (N)}$$

III.4.2 Number of Reynolds

The number of Reynolds (Re) is a dimensionless parameter that characterizes the flow regime of a fluid. It is defined as the ratio of inertial forces to viscous forces in the fluid, and it depends on the fluid density, viscosity, velocity, and characteristic length scale. The number of Reynolds can indicate whether the flow is laminar or turbulent, which affects the drag force and the lift force on the drone. In general, laminar flow has lower drag and higher lift than turbulent flow, but it is also more prone to separation and stall. Therefore, the design of the drone should consider the optimal range of Reynolds numbers for its intended operating conditions and performance goals.

To calculate the number of Reynolds for the drone, we can use the following formula:

$$Re = \frac{\rho V L}{\mu} \dots\dots\dots (10)$$

where:

- ρ is the density of the fluid = 1.225 (kg/m³)
- V is the flow speed (m/s) = 35 m/s
- L is a characteristic length (m) (in our case it will be the MAC length)= 0.301 m
- μ is the dynamic viscosity of the fluid = 1.81e-5 (Pa·s or N·s/m² or kg/(m·s))

In the previous chapter, we learned how to estimate the values of these parameters based on the geometry, mass, and power of the drone, as well as the properties of the ambient air. For example,

assuming a density of 1.225 kg/m³, a viscosity of 1.81e-5 Pa.s, a velocity of 35 m/s, and a length of 0.921 m, we obtain:

$$Re = 1.225 \times 35 \times 0.301 / 1.81e-5$$

$$Re = 713004 \text{ (no unit)}$$

This value indicates that the flow around the drone is highly turbulent, which implies a high drag coefficient and a low lift coefficient. To reduce the drag and increase the lift, the drone could have a more streamlined shape, a smaller size, or a lower speed. However, these changes may also affect the stability, maneuverability, and payload capacity of the drone. Therefore, the designer should balance the trade-offs between different design criteria and select the most suitable Reynolds number for the drone.

III.4.3 Weight force

we already of the total mass of the drone (12,5 kg plus 5kg payload), we can use the formula number (11) to calculate the weight:

$$W = M \times g \dots\dots\dots (11)$$

Where:

M: mass of the drone = 17.5 (kg)

g: force of gravity = 9,81 (m/s²)

$$W = 17.5 \times 9.81$$

$$W = 171.67 \text{ (N)}$$

III.4.4 Lift to Drag ratio

Lift and drag coefficients are normally determined experimentally using a wind tunnel. But for some simple geometries, they can be determined mathematically using [31]:

$$L/D = \frac{F_L}{F_D} = \frac{C_L}{C_D} \dots\dots\dots (12)$$

L/D: Lift to Drag ratio

F_L: Lift Force = 545.92 (N)

F_D: Drag force = 10.36 (N)

C_L: Coefficient of Lift = 0.79 (without a unit)

C_D: Coefficient of Drag = 0.015 (without a unit)

$$L/D = \frac{545.92}{10.36} = \frac{0.79}{0.015}$$

$$L/D = 52.66 \text{ (no unit)}$$

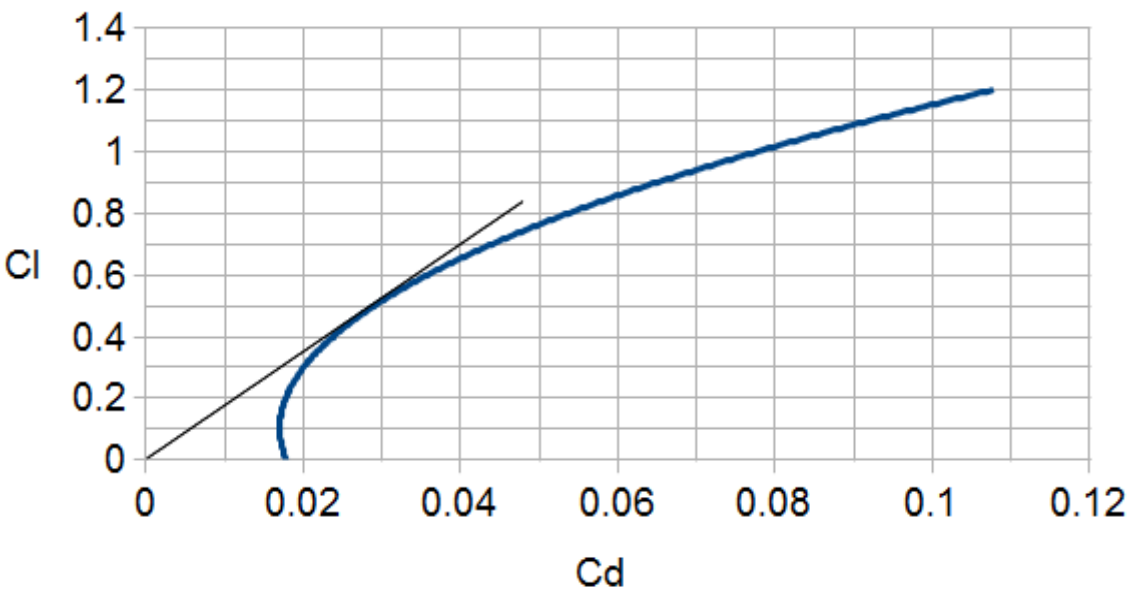


Figure III.5 Drag curve for light aircraft. The tangent gives the maximum L/D point [32]

The L/D ratio calculated earlier indicates the aerodynamic efficiency of the UAV. A higher L/D ratio means that the drone can travel farther with less drag and less energy loss. The L/D ratio of 52.66 is relatively high compared to typical values for other UAVs, which range from 10 to 30. This suggests that the projectile has a streamlined shape and a low coefficient of drag [32]. Another key factor in performance is speed, which determines how fast the aircraft can travel and how far it can reach. Speed also affects the aerodynamic forces and moments acting on the UAV, such as lift, drag, and stability. To analyze the speed of the drone, we need to consider its trajectory speed, which is the speed of the projectile relative to the surrounding air. Equation (13) shows how to calculate the trajectory speed based on the mass, gravity, density, area, and coefficients of lift and drag of the projectile [17].

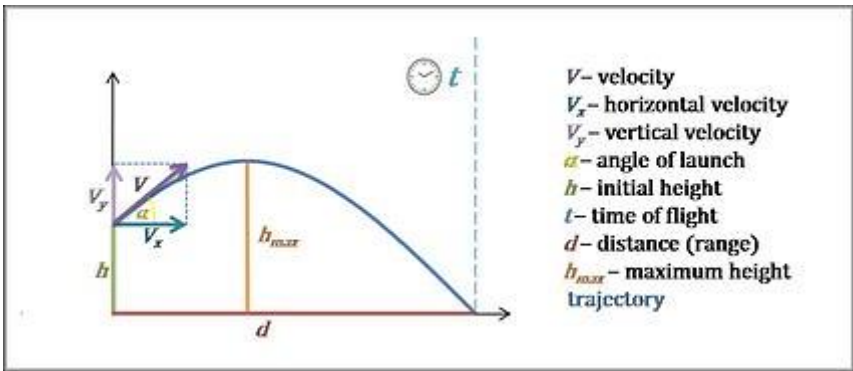


Figure III.6 Trajectory speed [33]

$$V_T = \sqrt{\frac{2Mg}{\rho A}} \times \sqrt{\frac{1}{C_L^2 + C_D^2}} \dots\dots\dots (13)$$

Where:

V_T : trajectory speed (m/s)

M : masse = 17.5 (kg)

g : gravity force 9,81 (m/s²)

ρ : density =1,225 (kg/m³)

A : Wing area = 0.921 (m²)

C_L, C_X : lift and drag coefficient (without a unit)

$$V_T = \sqrt{\frac{2 \times 17,5 \times 9,81}{1.225 \times 0.921} \times \frac{1}{0,79^2 + 0,015^2}}$$
$$V_T = 19.61 \text{ (m/s)}$$

The horizontal speed is obtained by using [15]:

$$V_H = V_t \times \cos(\arctan(\frac{C_L}{C_D})) = V_t \times \frac{C_L}{C_L + C_D} \dots\dots\dots (14)$$

V_H : horizontal speed (m/s)

V_T : vertical speed (m/s)

C_L, C_X : lift and drag coefficient (without a unit)

$$V_H = 19,61 \times \frac{0.79}{0.79 + 0,015}$$
$$V_H = 19.24 \text{ (m/s)}$$

III.4.5 AFT CG Limit

The Aft CG limit is the most rearward position of the center of gravity (CG) for which the aircraft meets the stability and control requirements. The aft CG limit depends on several factors, such as the wing loading, the tail size and shape, the elevator deflection, and the speed. If the CG is too far aft, the aircraft may become unstable and difficult to control, especially at low speeds or high angles of attack. The aft cg limit is usually determined by flight tests or simulations and is marked on the CG envelope diagram. However, we can calculate this position mathematically by applying equation (15):

$$ACGL = MAC \times (0.25 + V_s \times \frac{AR+2}{AR} \times \frac{ARs}{ARs+2}) \dots\dots\dots (15)$$

ACGL: Aft Center of Gravity Limit

MAC: mean aerodynamic chord = 0.301 (m)

V_s : stabilizer volume coefficient= 0.6 (no unit, the 0.6 value is already explained in chapter II)

AR: wing’s aspect ratio = 10.407 (without a unit)

ARs: stabilizer aspect ratio

To find the ACGL, we just need the stabilizer aspect ratio (ARs), which uses the same equation as the wing’s aspect ratio, equation (2):

$$AR = \frac{bs^2}{As}..... (2)$$

Where:

bs: stabilizer wingspan 0.931(m)

As: stabilizer area 0,184 (m²)

$$AR = \frac{0,931^2}{0,184}$$

$$AR = 4.7 \text{ (no unit)}$$

After calculating the stabilizer aspect ratio, we can now compute the ACGL:

$$ACGL = 0.301 \times (0.25 + 0.6 \times \frac{10.47+2}{10.47} \times \frac{4.7}{4.7+2})$$

$$ACGL = 0.226 \text{ (m)}$$

We will be resuming the second part of chapter III in the tables below:

Data	Value
Mass (M)	17.5 kg
Gravity (g)	9.81 m/s ²
Density (ρ)	1,225 kg/m ³
Speed (maximum speed used)	35 m/s
Angle of Attack	5 ⁰
C _L	0,79
C _D	0.015
Wing area (A)	0.921 m ²
Wing aspect ratio (AR)	10.47 (no unit)
Dynamic viscosity (μ)	1.81e-5 Pa.s
MAC	0,301 m
Wingspan (b)	3 m
V _s	0.6 (no unit)

Table III.4 Giving data for the calculation of the performance parameters

Calculated data	Value
Lift force (F _L)	545.92 N

Drag force (F_D)	10.36 N
Reynolds number	713004 (no unit)
Weight force (W)	171.67 N
L/D Ratio	52.66 (no unit)
Trajectory speed (V_T)	19.61 m/s
Horizontal speed (V_H)	19.24 m/s
Aft CG Limit	0,226 m

Table III.5 Calculated performance parameters of the 17.5 kg drone

Having meticulously navigated through the drone design process using the SPP method (Simple, Practical and Performant), we are now ready to delve into the core of our research. Our primary objective is to explore the impact of altering the drone’s mass on its size and performance. This involves a comprehensive analysis of how changes in mass influence various parameters such as lift, drag, speed, and maneuverability. To facilitate this, we will be using MATLAB, a powerful computational tool, to systematically vary the drone’s mass and observe the resulting changes in structural dimensions and performance. By leveraging MATLAB’s robust data analysis and visualization capabilities, we aim to derive insights that could potentially lead to the development of more efficient and versatile drones. This endeavor not only enhances our understanding of drone dynamics but also paves the way for innovative design strategies in the field of drone technology. Through this research, we aspire to contribute to the ongoing advancements in drone design and applications.

We will begin by picking a different mass, select any mass you prefer, whether it is bigger or smaller depending on the purpose of use of your drone. We will take a mass of 5.6 kg for example and study the new module using MATLAB and the calculating formulas already mentioned in this chapter and chapter number II.

MATLAB:

Before we proceed with the analysis, let us briefly introduce MATLAB and its features. MATLAB is a software platform that allows users to perform numerical computations, data manipulation, visualization, and programming. MATLAB stands for Matrix Laboratory, as it is designed to work with matrices and arrays of data. MATLAB has a user-friendly interface that enables users to interact with the software through commands, scripts, functions, and graphical tools. MATLAB also supports various toolboxes and libraries that extend its functionality and provide specialized tools for different domains, such as signal processing, image processing, optimization, machine learning, and robotics. MATLAB is widely used in academia and industry for research and development, as it offers a fast and flexible way to prototype and test algorithms and models. MATLAB is particularly suitable for our drone design project, as it allows us to easily implement the equations and formulas that govern the drone's behavior and performance, and to visualize the results in graphs and charts. MATLAB also enables us to run simulations and experiments with different parameters and scenarios, and to compare and evaluate the outcomes. By using MATLAB, we can gain a deeper understanding of the drone's dynamics and optimize its design according to our objectives and constraints [34].

III.5 Effect of mass change on performance

One of the factors that affects the performance of a drone is its mass, which determines how much thrust and power are required to lift and move the drone. The mass of a drone depends on the components and materials used to build it, as well as the payload that it carries. Changing the mass of a drone can have various impacts on its flight characteristics, such as stability, maneuverability, speed, endurance, and range. In this section, we will explore how changing the mass of our drone affects its performance, using MATLAB to perform the calculations and simulations. We will compare the results calculated earlier with a new drone of 5.6 kg mass and analyze the trade-offs and benefits of modifying the mass.

Calculated parameters	Value
Wing area	0.301 m ²
Aspect ratio	12.94 (no unit)
Wing loading	18.11 kg/m ²
MAC	0.159 m
L _{HT}	0.397 m
L _{VT}	0.4 m
Lift force (F _L)	183.15 N
Drag force (F _D)	3.47 N
Reynolds number	376636.74 (no unit)
Weight force (W)	54.936 N
L/D Ratio	52.78 (no unit)
Trajectory speed (V _T)	15.11 m/s
Horizontal speed (V _H)	14.72 m/s

Table III.6 Calculated performance parameters of the 5,6 kg drone

It is evident that using reduced mass leads to a lighter UAV, smaller in size, which needs less lift force to take off and creates less drag. We also observe that the weight force is almost a third of the weight force of 17.5 kg, which means that it will probably need less power and have a longer endurance.

However, using a lower mass and smaller size drone does not always imply that it will be beneficial, its drawbacks are less payload to be carried, long endurance demands more advanced electronic controllers or in other words more costly.

III.6 Effects of Taper Ratio on Aerodynamic Parameters of fixed wing Drone

An aircraft designer has so many tasks to overcome during an aircraft design process. One of the most important tasks is to design an efficient wing complying with the determined requirements. This is generally possible by optimizing so many geometrical and aerodynamic parameters of the wing [35]. Geometrically, airfoil and planform geometries are the main terms

to define a wing. An aerodynamically efficient wing can be designed when the suitable airfoil(s) and planform geometry coupled. Therefore, planform geometry is one of the most important geometries during an aircraft design process. Taper ratio is one of the parameters on planform geometry which means the ratio of the root and tip chord lengths of a wing. Hence, its effects on wing’s aerodynamic parameters are also important and should be taken into consideration during a wing design process [36] [37].

The effects of the taper ratio on wing aerodynamic parameters can be obtained by means of numerical or experimental analyses [38]. At the conceptual design phase of an aircraft, it can be preferable to use computational fluid dynamics programs rather than time consuming experimental setups. There are so many programs to perform these analyses such as Ansys Fluent, MATLAB and SolidWorks Flow Simulation. In the literature, including numerical analyses, there are so many studies investigating the aerodynamic parameters of aircraft wings.

III.6.1 Material and method

a- Planform Geometry and Aerodynamic Parameters of an Aircraft Wing

Planform geometry is the top-view shape of a wing and effective on wing aerodynamic performance [39] [40]. Therefore, the geometrical parameters of a wing planform geometry are also important for a wing design. Changing these geometrical parameters properly with respect to their effects on the wing aerodynamic parameters can provide an improved aerodynamic performance to wing. Taper ratio (λ), as a part of the wing planform geometry, is one of these important parameters to take into consideration during an aircraft wing design process. It is the ratio as stated in Equation (16), which is the ratio of the root (C_r) and tip (C_t) chord lengths as shown in Figure III.7.

$$\lambda = \frac{C_t}{C_r}..... (16)$$

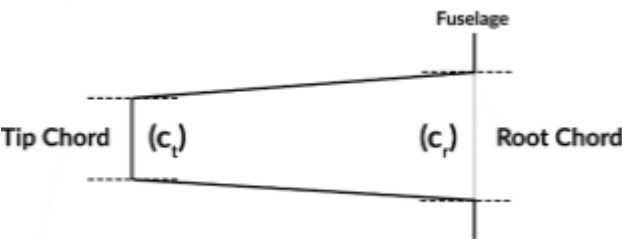


Figure III.7 Aircraft wing root and tip chords

The main aerodynamic parameters of an aircraft wing are drag (C_D), lift (C_L) and pitching moment (C_M) coefficients. The other aerodynamic performance parameters can be derived from these parameters, such as glide ratio, which is the ratio between lift coefficient and drag coefficients. Lift, drag and pitching moment coefficients can be calculated using the Equations (17) - (18) - (19). In these equations, A is the related area (m^2), V is the freestream velocity (m/s), F_L is the lift force (N), F_D is the drag force (N) and F_M is the moment (Nm).

$$C_L = \frac{0.5 \cdot A \cdot V^2}{F_L}..... (17)$$

$$C_D = \frac{0.5 \cdot A \cdot V^2}{F_D} \dots\dots\dots (18)$$

$$C_M = \frac{0.5 \cdot A \cdot V^2}{F_M} \dots\dots\dots (19)$$

Oswald efficiency factor (e) is the value, which gives an idea about the similarity of a wing’s span-wise lift distribution to the elliptical lift distribution. The elliptical lift distribution has an Oswald efficiency factor of 1 and generally this is the maximum value of this parameter. There is another single parameter, which can represent wing efficiency in terms of induced drag, named as induced drag parameter (δ) and can be calculated from Equation (20) [41]. This parameter depends only on planform geometry and independent from angle of attack and lift coefficient.

$$e = \frac{1}{1+\delta} \dots\dots\dots (20)$$

$$C_{Di} = \frac{C_L^2}{AR \times \pi \times e} \dots\dots\dots (21)$$

b- Numerical Analyses

The main objective of this study is to investigate the effects of taper ratio on aerodynamic parameters of a wing design. In order to examine the effects, taper ratio was revised to 0.2, 0.4, 0.62, 0.8 and 1.2 by changing tip and root chord lengths while keeping wing area, aspect ratio and mean geometric chord (M.A.C.) values constant, as shown in Figure III.8.

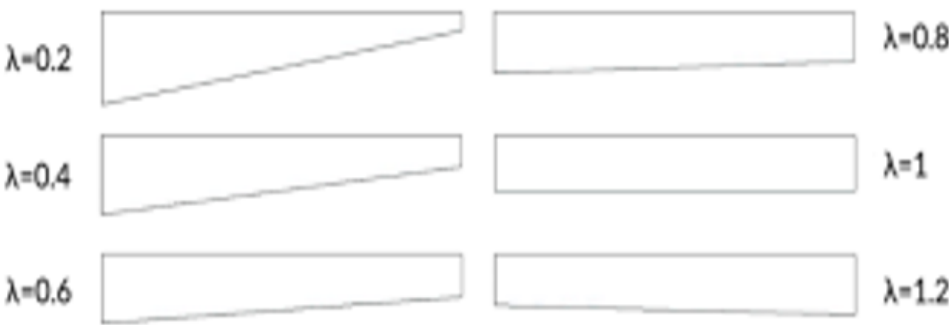


Figure III.8 Planform geometries of revised wing models [44]

Numerical analyses of the six different wing models were performed by MATLAB program. The geometrical dimensions of the models were given in Table III.7.

Model	Root Chord (m)	Tip Chord (m)	M.A.C (m)	Wing Area (m ²)	Aspect Ratio	Taper Ratio
1	0.078	0.016	0.047	0.037	16.6	0.2
2	0.067	0.027				0.4
3	0.058	0.036				0.62
4	0.052	0.042				0.8
5	0.047	0.047				1
6	0.043	0.051				1.2

Table III.7 Geometrical dimensions of the models [45]

Lastly, the models revised from the baseline rectangular wing model were numerically analyzed at different Reynolds Number. As all the models have high aspect ratios, which is common on sailplane wing designs, the airspeed was used is 33.5m/s as a typical sailplane cruise speed [42] [43]. As the stall condition angle of attack or higher values are not scope of this study. [35] [44].

c- Results and discussion

The results of numerical analyses performed on MATLAB program at different Reynolds Number in terms of the wingspan 3.096 m of the six models were given in Table III.7. For four values of total mass of the fixed wing Drone. Figure III.9 presents the effect of Taper Ratio on the Reynolds number. We notice that the Reynolds number decreases if λ increases. The relationship between these two parameters is non-linear. On the other hand, if the total mass of drone increases, we notice that the Reynolds number also increases.

Figure III.10 presents the numerical analysis results of the models in terms of the induced drag parameter. It appears that (δ) grows with an increase of Taper ratio, this case was calculated with $AR=16.6$. Both İbrahim Halil Güzelbey's data [45] and the present data indicate that induced drag is the smallest for a taper ratio with a value of 0.4. Also, the trends of the present calculation follow the same trend exhibited by the data for the smaller AR wing,[46] (e.g., increasing towards the small or the large taper values) (Figure III.11). This is expected since at the extremely low taper ratios high wing tip loading results, causing the spanwise loading shape to be far from elliptic. Similarly, at the high taper ratio values wing root has a high load and wing tip is unloaded, again deviating from the elliptic shape.

in Figure III.12, the numerical results for induced drag coefficients changing with taper ratios of the models were given. As expected, the change of induced drag coefficient values is in good agreement with the values of induced drag parameter. Model 2 ($\lambda=0.4$) has the minimum ($=0.00543$) and model 6 ($\lambda=1.2$) has the maximum value ($=0.005886$) of induced drag coefficient. Model 1, 3, 4 and 5 have induced drag values of 0.005449, 0.005488, 0.005622 and 0.005806, respectively. These results are compared with İbrahim Halil Güzelbey [45] and Tommy M. Chen and Joseph [46] results.

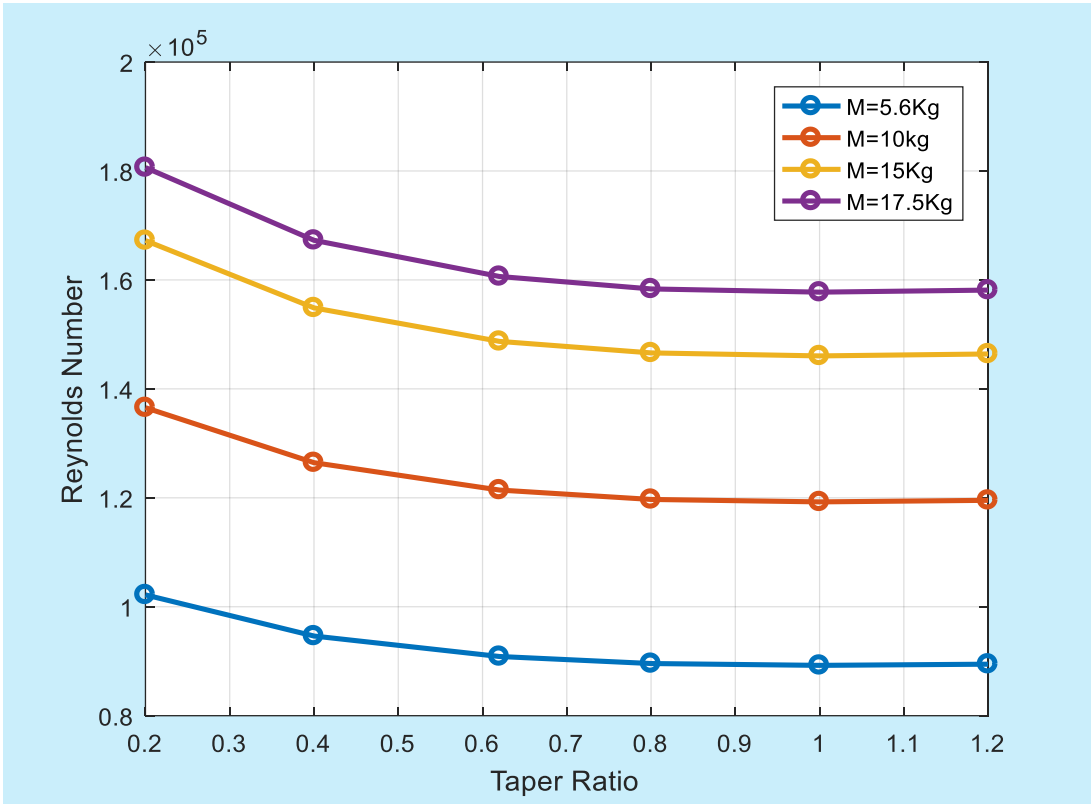


Figure III.9 Reynolds Number versus taper ratios of the models

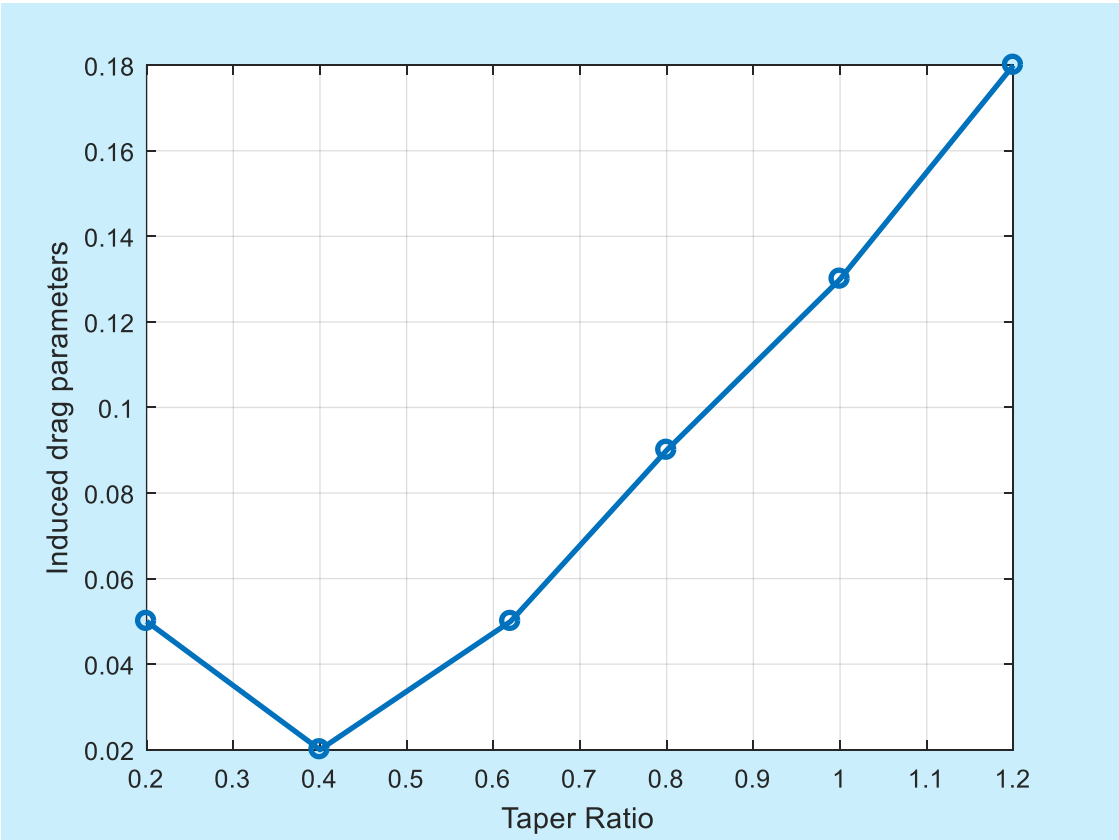


Figure III.10 Induced drag parameters (δ) versus taper ratios of the models

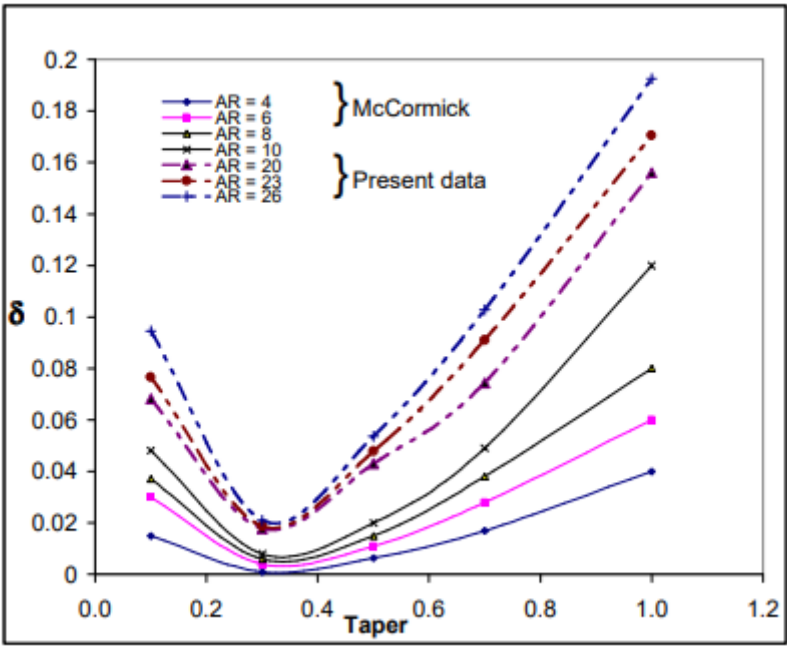


Figure III.11 Induced drag parameter versus taper ratio and aspect ratio [46]

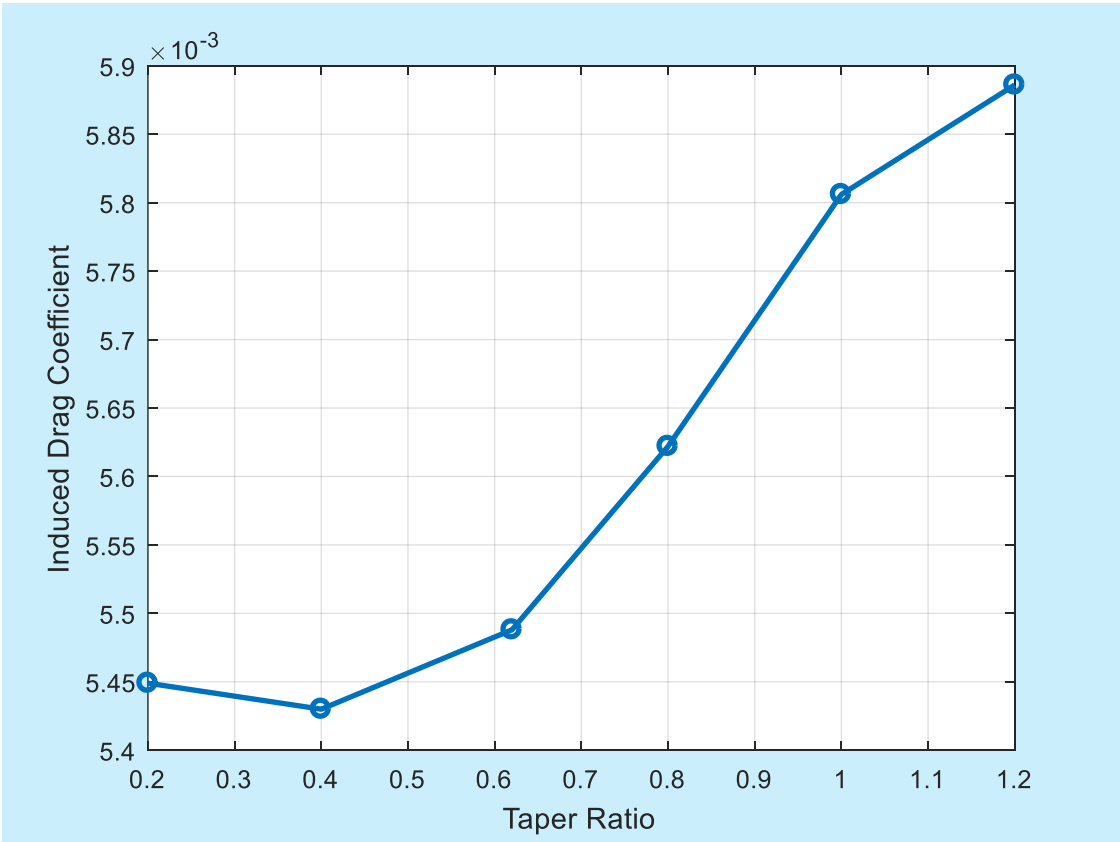


Figure III.12 Induced drag coefficients versus taper ratios of the models

III.6.221 Conclusion

In conclusion, this chapter provided a comprehensive study of the fixed-wing drone, specifically the SkyEye Sierra model. We began by calculating various parameters such as structural, performance, and aerodynamic characteristics, assuming a fixed mass of 17.5 kg. This initial analysis offered valuable insights into the drone's capabilities and performance under these specific conditions. However, recognizing that mass is a variable parameter in real-world scenarios, we proceeded to change the mass and recalculate all the parameters. This exercise demonstrated the significant impact of mass on the drone's performance and structural parameters, emphasizing the importance of accurate mass estimation in drone design and operation.

Furthermore, we delved into the study of the taper ratio's effect on wing design and its subsequent influence on aerodynamic parameters. Specifically, we examined its impact on the Reynold number and induced drag. This investigation highlighted the critical role of taper ratio in optimizing wing design for improved aerodynamic efficiency.

Overall, this chapter underscores the intricate interplay of various factors in drone design and operation. The findings from our study of the SkyEye Sierra model serve as a valuable reference for future drone design and research.

Organizational Chart

The following organizational is a visual representation of the systematic approach taken to develop a MATLAB program for UAV design. Let us delve into each step to understand the workflow and the interdependencies of the parameters involved.

Starting Point: Equations and Mass

The journey begins with the transcription of equations from the thesis's second chapter into MATLAB. These equations form the backbone of the UAV's design, encompassing structural and aerodynamic principles. The mass of the UAV is introduced as a variable factor, which is a critical aspect since it influences numerous design parameters. In aerodynamics, mass affects the lift required for flight and, consequently, the size and shape of the wings and other components.

Taper Ratio's Influence

Following the initial setup, the program examines the taper ratio and that is the change in wing's chord from the root to the tip. This parameter is crucial as it affects the UAV's performance, particularly its aerodynamic efficiency and stability. A higher taper ratio can reduce drag but may also impact stability, requiring careful consideration during the design phase.

Iterative Design Process

The chart outlines an iterative design process that includes:

First Draft: Creating a preliminary design based on the initial parameters and equations.

Flight Dynamics: Analyzing how the UAV will behave in flight, considering forces such as lift, drag, and moments that will act upon it.

Update Design: Refining the design iteratively based on the flight dynamics analysis to optimize performance and stability.

Design Parameters and Their Interplay

The program takes the input drone mass and calculates several interrelated parameters:

Wing Area (A): Determines the amount of lift that can be generated.

Aspect Ratio (AR): Affects the lift-to-drag ratio and wing efficiency.

Induced Drag Coefficient : Represents the drag due to lift and is influenced by the aspect ratio.

Mean Aerodynamic Chord (MAC): The average chord length, which is vital for locating the center of pressure.

Lift/Drag Ratio: A key performance indicator that influences the UAV's range and endurance.

Takeoff Weight (TO): The total weight of the UAV, which must be supported by the lift generated.

Final Outcomes: Stability and Performance

The program's output includes crucial measurements for stability:

Length between the Aerodynamic Centers of the Wing and Vertical Tailplane: This distance is essential for yaw stability.

Length between the Aerodynamic Centers of the Wing and Horizontal Tailplane: This measurement is significant for pitch stability.

Conclusion of the Program

The program concludes with a set of optimized design parameters that ensure the UAV's performance meets the desired specifications. The end result is a UAV design that is balanced in terms of aerodynamics, stability, and performance, ready to be further developed and tested.

This organizational chart encapsulates the essence of our thesis work, highlighting the critical role of MATLAB in the design and optimization of UAVs. It reflects a comprehensive study that integrates theoretical knowledge with practical application, paving the way for the development of sophisticated drones.

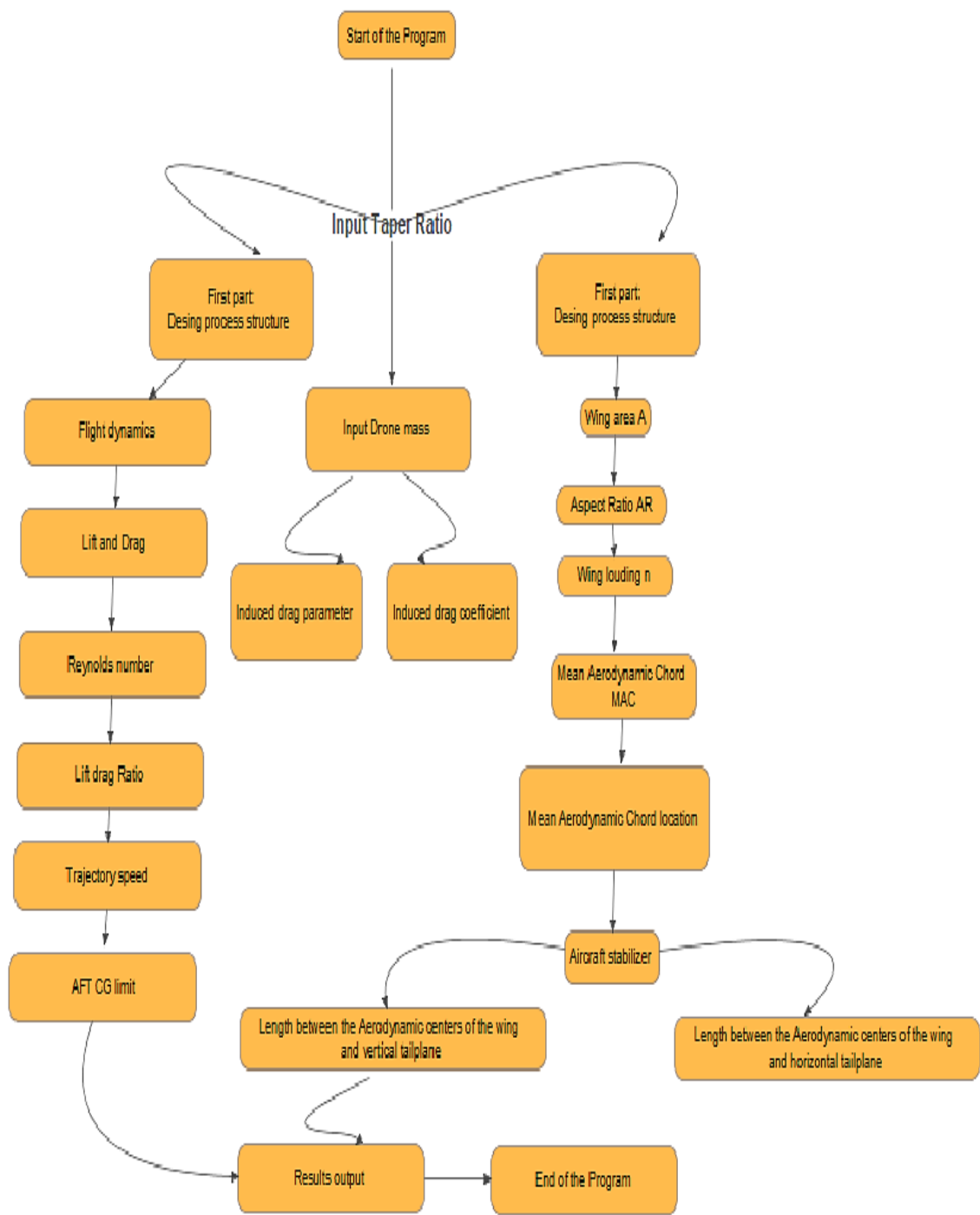


Figure III.13 Organizational Chart of the MATLAB program

SolidWorks Drawings

SolidWorks is a powerful 3D CAD (Computer-Aided Design) software that is widely used in various industries for product design, simulation, and manufacturing. Founded in 1995, SolidWorks allows designers to sketch out ideas, experiment with features and dimensions, and produce models and detailed drawings [47].

The software is component-based, meaning it allows you to build parts in a virtual environment and then assemble them to create complex 3D models [47]. It also supports a variety of features such as parametric design, surface modeling, and geometric analysis [48]. These features make SolidWorks an excellent tool for designing intricate objects like drones.

For our project, we will be using SolidWorks combined with the data we have gathered from our previous work. We will design a fixed-wing drone, taking into account various parameters such as aerodynamics, weight, and balance. SolidWorks will allow us to visualize the drone from different views and angles, ensuring a comprehensive design process.

In addition to designing the drone, SolidWorks will also enable us to run simulations to test the drone’s performance under different conditions. This will help us optimize the drone’s design and ensure it meets our objectives and constraints [47].

By using SolidWorks, we can streamline our design process, improve accuracy, and ultimately create a more effective and efficient drone [48].

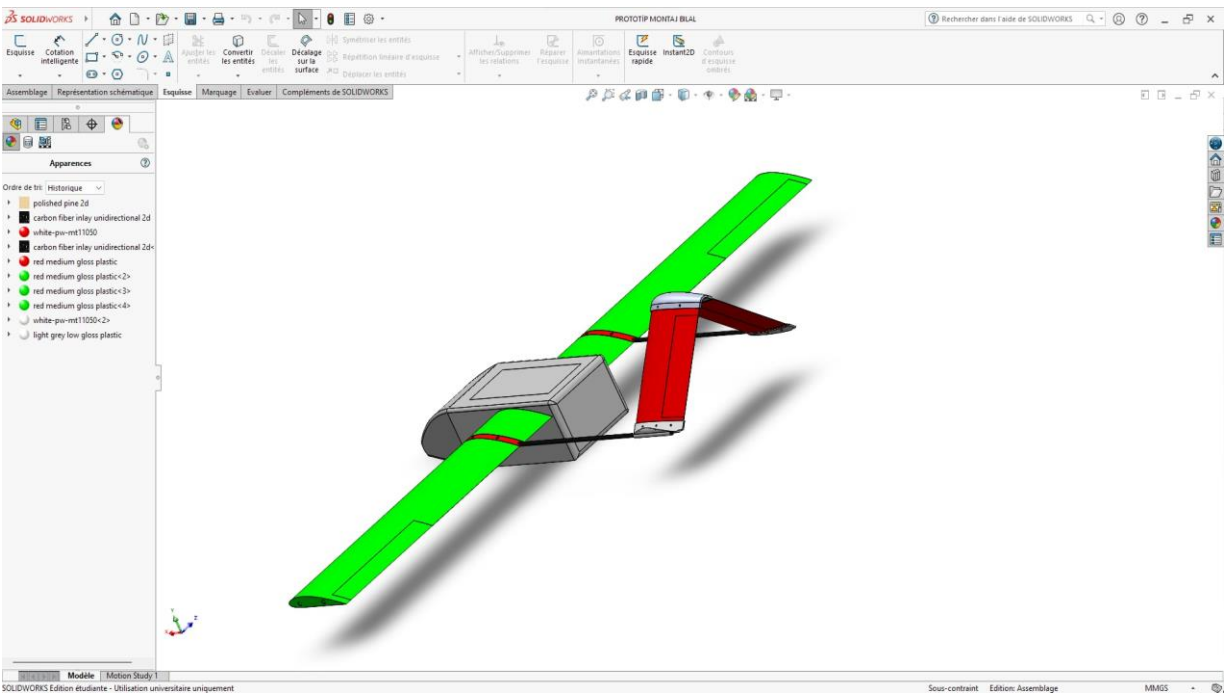


Figure III.14 3D back view of the designed drone

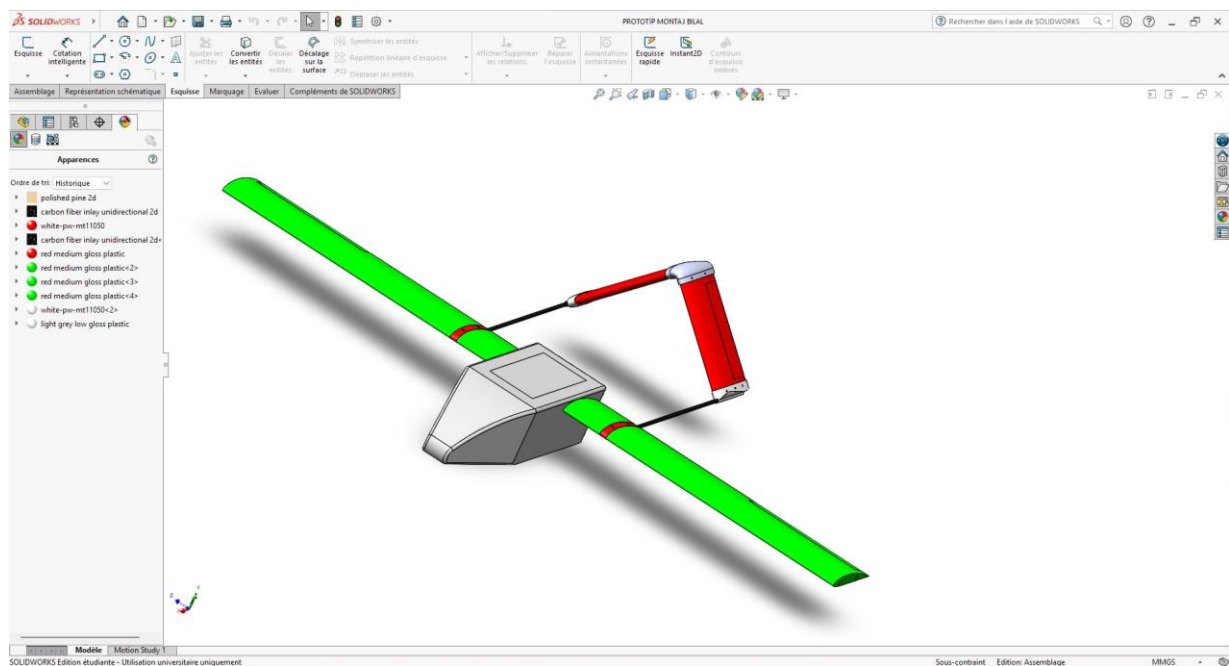


Figure III.15 3D front view of the designed drone

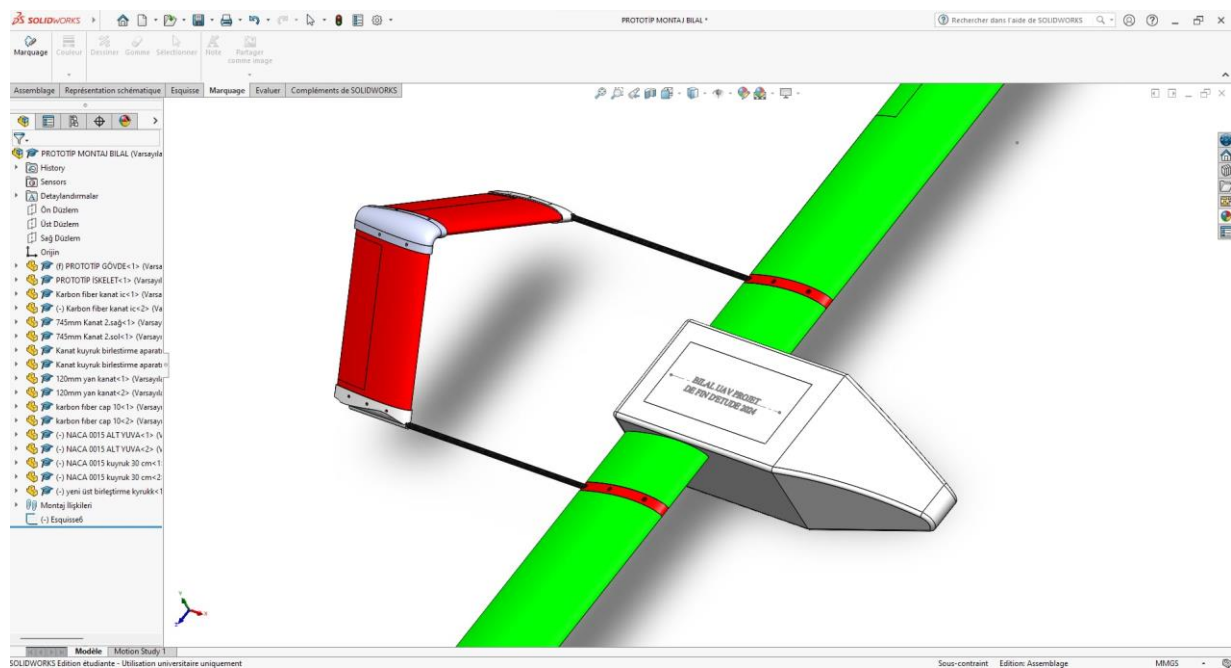
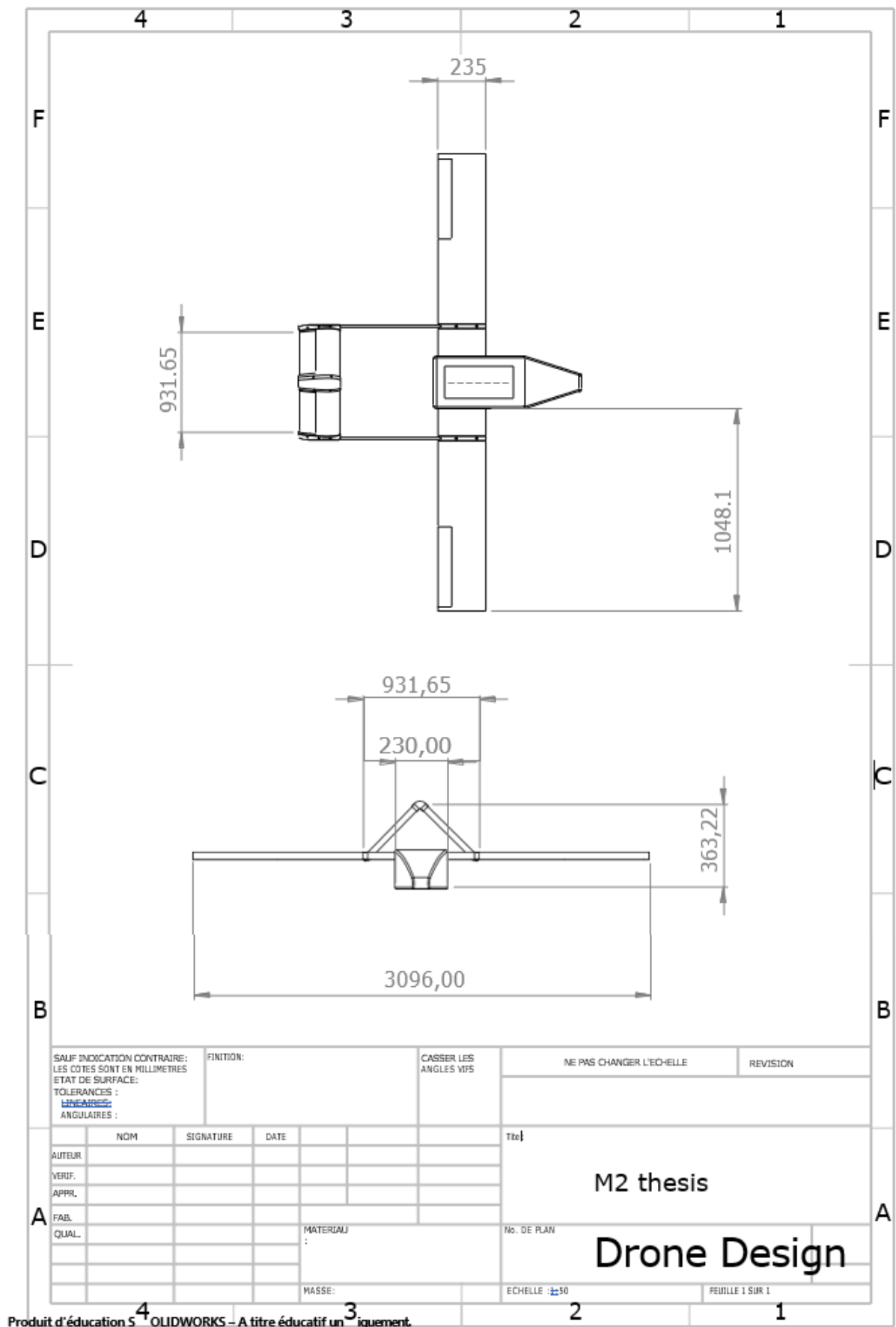
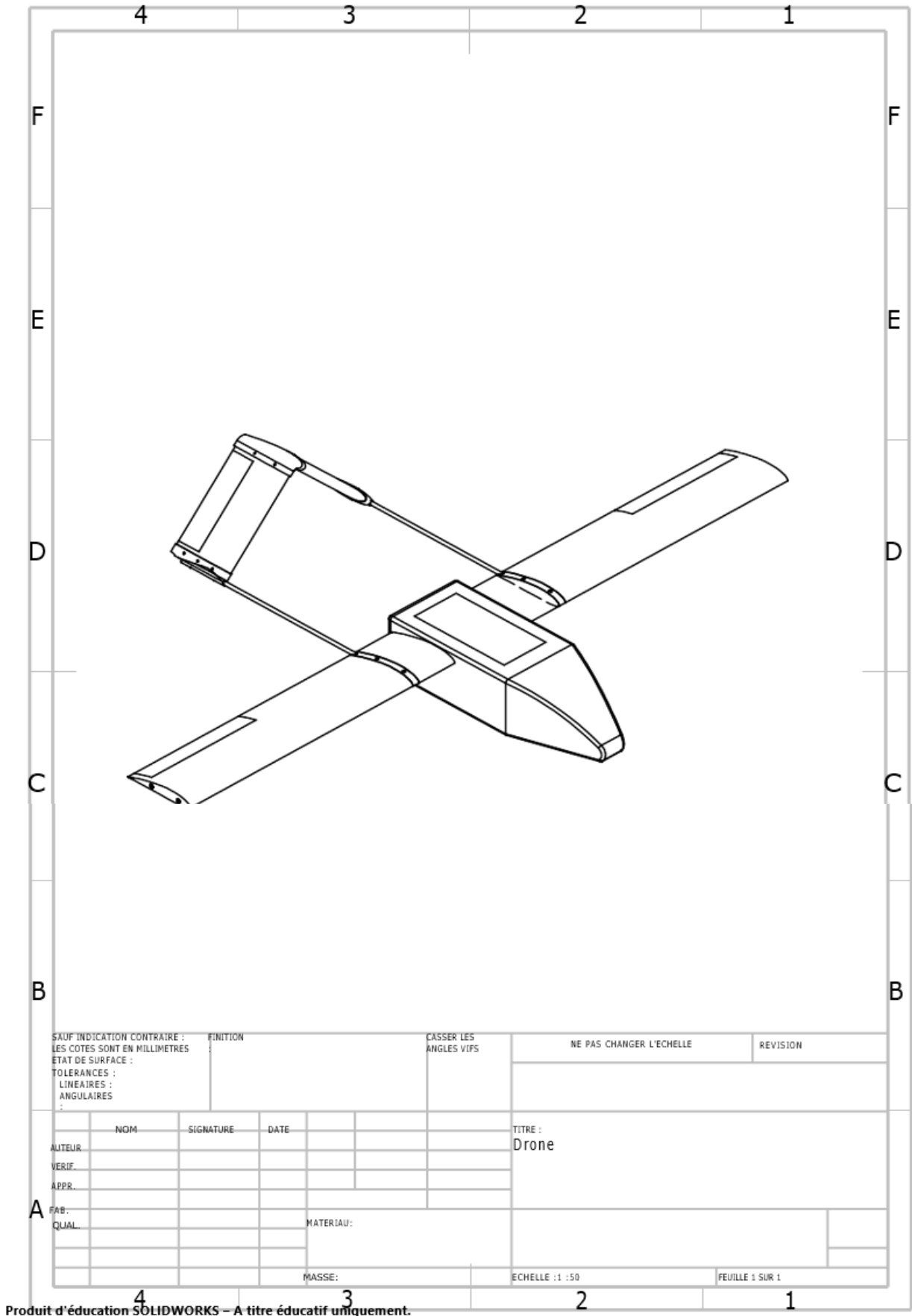


Figure III.16 3D upper view of the designed drone





General Conclusion

General Conclusion

This master's thesis has delved into the use of MATLAB for the calculation and design of drones of varying scales, providing a comprehensive exploration of the topic.

Chapter I served as an introduction to the world of drones. We discussed the history of drones, tracing their evolution from simple unmanned aerial vehicles to the sophisticated machines we see today. We also explored the various applications of drones, highlighting their versatility and the wide range of industries they have impacted, from agriculture and construction to surveillance and delivery services. This chapter underscored the importance of drones in our modern world and set the stage for the technical discussions that followed.

In Chapter II, we revisited the mathematical principles underlying drone design. We went through various formulas used to calculate the structural and aerodynamic parameters of a drone, such as lift, drag, and stability. This chapter served as a refresher on the theoretical aspects of drone design, emphasizing the importance of understanding these principles when designing efficient and effective drones.

Chapter III was where we put theory into practice. Using MATLAB, we calculated the parameters of a drone with an initial mass of 17.5 kg. We then altered the mass to 5.6 kg in the MATLAB program to observe the changes in the drone's parameters. This exercise demonstrated the power of MATLAB as a tool for drone design, allowing us to easily simulate different drone designs and instantly see the effects of changing various parameters.

We also studied the effect of the taper ratio on the aerodynamic parameters of the wing using MATLAB. The taper ratio, which is the ratio of the tip chord to the root chord of the wing, is a critical factor in determining the aerodynamic performance of a drone. Our investigation revealed that changes in the taper ratio can significantly affect the lift-to-drag ratio, stall characteristics, and overall aerodynamic efficiency of the drone.

This thesis has shown that MATLAB is an invaluable tool for drone design. Its ability to perform complex calculations quickly and accurately, coupled with its flexibility in handling different design parameters, makes it an ideal tool for drone designers. As drones continue to grow in importance and application, tools like MATLAB will undoubtedly play a crucial role in driving innovation in drone design.

The findings of this thesis have significant implications for both academia and industry. For researchers, this work contributes to the growing body of knowledge on drone design and highlights the potential of computational tools like MATLAB in advancing this field. For practitioners, the insights gained from this research can inform their design practices, helping them create more efficient and effective drones.

Looking ahead, there are several avenues for future research. One could extend this work to include other design parameters, such as wing loading, aspect ratio, and propeller design, and explore their impact on drone performance. Additionally, one could investigate the use of other computational tools for drone design and compare their effectiveness with MATLAB.

In conclusion, this thesis has not only deepened our understanding of drone design but also highlighted the potential of MATLAB as a tool for innovation in this field. It is hoped that this

work will inspire further research and innovation in drone design, contributing to the advancement of this exciting field.

References

- [1] Barnhart, R. K., Marshall, D. M., & Shappee, E., Introduction to unmanned aircraft systems, 2021.
- [2] Hall, O. & Wahab, The use of drones in the spatial social sciences, 2021.
- [3] published by the royal British museum of art, www.Wikipedia.com.
- [4] Mohsan, S. A. H., Khan, M. A., Noor, F., Ullah, I., & Alsharif, M. H, Towards the unmanned aerial vehicles (UAVs): A comprehensive review. Drones, 2022.
- [5] Benarbia, T. & Kyamakya, K, A literature review of drone-based package delivery logistics systems and their implementation feasibility. Sustainability., 2021.
- [6] Constantine Samaras and Joshua Stolaroff, The Conversation Smithsonian magazine, 2018.
- [7] Leon Amadeus Varga, Benjamin Kiefer, Martin Messmer, and Andreas Zell. "Seadronessee: A maritime benchmark for detecting humans in open water". In Proceedings of the IEEE/CVF winter conference on applications of computer vision, pages 2260–2270, 2022.
- [8] <https://enterprise-insights.dji.com/blog>," Why SAR teams are turning to drones to help save lives", 2021.
- [9] <https://visionaerial.com/successful-drone-search-and-rescue-missions>, 2022.
- [10] Meivel, S. & Maheswari, S. "Remote sensing analysis of agricultural drone". Journal of the Indian Society of Remote Sensing, 2021.
- [11] <https://adore.ifrc.org> /Algeria Fire - IFRC 2023.
- [12] <https://defensebridge.com/article/fixed-wing-drone>.
- [13] https://www.researchgate.net/figure/Rotary-wing-drones-Anonymous-2020c_fig3_366204592
- [14] <https://www.dji.com/global>, Phantom 4
- [15] https://www.google.com/search?q=Hubsan+X4++drone&sca_
- [16] <https://umilesgroup.com/en/types-of-drones-classification-by-use-and-characteristics/>
- [17] Azza Garbouj, SPP METHOD DESIGN OF A MODEL GLIDER OR AIRCRAFT, translated and published on Academia.com.
- [18] <https://aviation.stackexchange.com/questions/57436/does-a-deflecting-control-surface-change-the-wing-area>.
- [19] Andrew Wood, Fundamentals of Aircraft Design, September 2022.

- [20] Tomáš Vogeltanz, Application for calculation of mean aerodynamic chord of arbitrary wing planform, *AIP Conf. Proc.* 1738, 120018, 2016.
- [21] Priyanka Barua, Tahir Sousa & Dieter Scholz, “Empennage Statistics and Sizing Methods for Dorsal Fins” written at the Hamburg University of Applied Sciences (p51-53), 2013
- [22] <https://sciencebehindsuperpowers.weebly.com/flight.html>
- [23] <http://airfoiltools.com/airfoil/naca4digit>
- [24] www.faa.gov, FAA Pilot’s Handbook of Aeronautical Knowledge Chapter 5 Aerodynamics of Flight.
- [25] http://wikipedia.org/wiki/Lift-to-drag_ratio.
- [26] Michael V. Cook BSc, in Flight Dynamics Principles (Third Edition), 2013
- [27] <https://www.aeroexpo.online/prod/elevonx/product-187219-69645>
- [28] http://www.mdp.eng.cam.ac.uk/web/library/enginfo/aerothermal_dvd_only/aero/perf/perf_ac.html
- [29] https://www.airfieldmodels.com/information_source/math_and_science_of_model_aircraft/formulas/mean_aerodynamic_chord.htm#:~:text=To%20Locate%20the%20Mean%20Aerodynamic,rearward%20from%20the%20trailing%20edge.
- [30] <https://skill-lync.com/student-projects/flow-over-an-airfoil-37>
- [31] <https://www1.grc.nasa.gov/beginners-guide-to-aeronautics/lift-to-drag-ratio/#:~:text=Aerodynamicists%20call%20the%20lift%20to,can%20carry%20a%20large%20payload>.
- [32] https://en.wikipedia.org/wiki/Lift-to-drag_ratio
- [33] <https://www.omnicalculator.com/physics/trajectory-projectile-motion>
- [34] https://www.mathworks.com/products/matlab.html?s_tid=hp_products_matlab
- [35] Gudmundsson, S., General aviation aircraft design: Applied Methods and Procedures. 2013: Butterworth-Heinemann.
- [36] Raymer, D.P., Aircraft design: a conceptual approach, AIAA Education Series. Reston, Virginia, 2012.
- [37] Sadraey, M.H., Aircraft design: “A systems engineering approach”. 2012: John Wiley & Sons.
- [38] Bergmann, A., A. Huebner, and T. Loeser, “Experimental and numerical research on the aerodynamics of unsteady moving aircraft”. *Progress in Aerospace Sciences* 44(2): p. 121-137, 2008.
- [39] Wakayama, S. and I. Kroo, Subsonic wing planform design using multidisciplinary optimization. *Journal of Aircraft*, 1995. 32(4): p. 746-753.

- [40] Nelson, C. Effects of wing planform on HSCT off-design aerodynamics. in 10th Applied Aerodynamics Conference. 1992.
- [41] Chen, T. and J. Katz. "Induced Drag of High-Aspect Ratio Wings". in 42nd AIAA Aerospace Sciences Meeting and Exhibit. Doi:10.2514/6.2004-38. 2004.
- [42] Thomas, F. and J. Milgram, Fundamentals of sailplane design. Vol. 3: College Park Press College Park, Maryland. 1999.
- [43] Administration, F.A., "Glider Flying Handbook", Skyhorse Publishing Inc. 2007.
- [44] Frati, S., The Glider. Editore Ulrico Hoepli Milano, Milan, Italy, 1946
- [45] İbrahim Halil Güzelbey, Yüksel Eraslan, Mehmet Hanifi Doğru, "Effects of Taper Ratio on Aircraft Wing Aerodynamic Parameters": A Comparative Study, 3rd International Mediterranean Science and Engineering Congress (IMSEC 2018)
- [46] Tommy M. Chen and Joseph Katz, Induced Drag of High-Aspect Ratio Wings, Conference Paper · January 2004
- [47] https://my.solidworks.com/solidworks/guide/SOLIDWORKS_Introduction_EN.pdf
- [48] <https://www.solidworks.com/solution/3dexperience-solidworks-makers/cad-drone-software>